FACULTY OF TEXTILE ENGINEERING TUL

Dissertation Thesis

Tensile Characterization of Compression Sock's Ankle Cut-strips and Development of Models to Approximate the Laplace's Law

Study programme: P3106 Textile Engineering
Study branch: Textile Technics and Materials Engineering

Author: **Hafiz Faisal Siddique, M.Sc.**
Thesis Supervisor: Ing. Adnan Ahmed Mazari, Ph.D.
Department of Clothing technologies

Liberec 2023

Declaration

I hereby certify, I, myself, have written my dissertation as an original and primary work using the literature listed below and consulting it with my thesis supervisor and my thesis counsellor.

I acknowledge that my dissertation is fully governed by Act No. 121/2000 Coll., the Copyright Act, in particular Article 60 – School Work.

I acknowledge that the Technical University of Liberec does not infringe my copyrights by using my dissertation for internal purposes of the Technical University of Liberec.

I am aware of my obligation to inform the Technical University of Liberec on having used or granted license to use the results of my dissertation; in such a case the Technical University of Liberec may require reimbursement of the costs incurred for creating the result up to their actual amount.

At the same time, I honestly declare that the text of the printed version of my dissertation is identical with the text of the electronic version uploaded into the IS/STAG.

I acknowledge that the Technical University of Liberec will make my dissertation public in accordance with paragraph 47b of Act No. 111/1998 Coll., on Higher Education Institutions and on Amendment to Other Acts (the Higher Education Act), as amended.

I am aware of the consequences which may under the Higher Education Act result from a breach of this declaration.

March 10, 2023 Hafiz Faisal Siddique, M.Sc.

Acknowledgments

I set my earnest thanks before ALLAH, The Almighty, The Creator, The Most Beneficent, and The Merciful.

I am highly obliged and thankful to the administration of the Technical University of Liberec to offer me admission to Ph.D. and provide me with the facilities to live in the Czech Republic, study, and receive the doctorate.

I recognize the Technical University of Liberec through **prof. Dr. Ing. Zdeněk Kůs**, the symbol of kindness and knowledge. His support, guidance, and valuable suggestions helped me throughout this research work. I thank him from my heart and well wish for his life and prosperity.

I am thankful to my supervisor **Ing. Adnan Ahmed Mazari, Ph.D**., for their continuous support and guidance. I also thank, to **prof. Ing. Jiří Militký, CSc., doc. Ing. Lukáš Čapek Ph.D**., whose expertise was quite helpful in formulating the research work.

I am thankful to all the departments of TUL who helped and supported me to complete my work. I am much thankful to doc. Ing. Vladimír Bajzík Ph.D., doc. Ing. Maroš Tunák Ph.D., and Ing. Michal Chotěbor for their support and help in measurements in the laboratory.

I want to say many thanks to Dean of faculty of textile engineering doc. Ing. Vladimír Bajzík Ph.D., Vice Dean, Ing. Iva Mertová, Ph.D., Ing. Hana Musilová, and Bohumila Keilová for looking after and caring for our documentation and academic affairs. Their kind guidance helped me a lot. I wish them prosperity and goodwill.

I would particularly like to say a special thanks to **Prof. Dr. Lijing Wang** (RMIT University, Australia), and **Prof. Dr. Lyndon Arnold** (RMIT University, Australia) for inviting me to their labs for the internship.

My gratitude will remain deficient if I do not name the contribution of my most sincere friends Dr. Musaddaq Azeem (Department of Material Engineering) and Dr. Abdul Jabbar (Assistant Professor, National Textile University, Pakistan)

Finally, I would like to dedicate my research and all relevant rewards to my mother and father (my hero and mentor), sisters, brothers, and especially my wife and newcomer Mr. Abdul Ahad Siddique for their encouragement, and prayers to complete this dissertation.

Hafiz Faisal Siddique

DEDICATION

DEDICATED TO MY GREAT AND BELOVED PARENTS ESPECIALLY MY MENTOR, TEACHER AND LEADER WHOSE COUNTLESS EFFORTS AND PRAYERS ARE THE BASIS OF MY SUCCESS

Abstract

Tensile properties of compression socks play a vital role to exert the adequate radial pressure, directly linked to their work performance, and working life. These properties are deployed using various type of materials and machine adjustments. In this scientific research work, socks samples were commercially bought and cut to evaluate their physical, structural, tensile properties and theory of exertion of compression pressure. So, current research work is comprised of two parts. Part 1 presents a scientific tensile characterization of the sock's cut-strip hauled to analyze; force at practical extension compared to experimental pressure (Ps), comparison between tensile indices, experimental pressure (Ps) and force at practical extension. These tensile indices include; loading energy (W), unloading energy (W′), hysteresis (H), and tensile linearity (TL). Results showed that the force value at practical extension (F_L) impart the significant influence to explain experimental pressure (Ps). It was also concluded that the tensile indices (W, W′, H, and TL) statistically shows significancy (R^2- value = moderate-strong) to force at practical and experimental pressure. Part 2 is comprised of a theoretical investigation of compression pressure using the modelization technique and transformation of the Laplace's law. This technique helped to explore some unknown parameters especially, deformed width (w_f), true stress (σ_T)/ logarithmic strain (ε_T)/true modulus (E_T). Using these unknown parameters; Laplace's law was transformed to two new mathematical models; Model 1 (T.Y.M); based on true Young's modulus and Model 2 (E.Y.M); based on engineering Young's modulus and deformed width (w_f). Furthermore, the results revealed that the transformed models; model 1 and model 2 and basic Laplace's law have well approximation to experimental pressure (Ps). Existing models were also compared to experimental pressure to analyze their efficacy. Newly transformed models were also statistically compared to original Laplace's law revealed that newly developed models have strong significant approximation to basic Laplace's law.

Keywords: *Tensile characterization, ankle cut-strips, modelization technique, transformed Laplace's laws, experimental pressure, approximation to Laplace's law*

Abstrakt

Tahové vlastnosti kompresních ponožek hrají zásadní roli při vyvíjení přiměřeného radiálního tlaku, přímo spojeného s jejich pracovním výkonem a životností. Tyto vlastnosti jsou nasazovány pomocí různých druhů materiálů a strojních úprav. V této vědecko-výzkumné práci byly komerčně zakoupeny a nařezány vzorky ponožek, aby se vyhodnotily jejich fyzikální, strukturální a tahové vlastnosti a teorie vyvíjení kompresního tlaku. Současná výzkumná práce se tedy skládá ze dvou částí. Část 1 představuje vědeckou charakteristiku tahu proužku ponožky taženého k analýze, sílu při praktickém vytažení ve srovnání s experimentálním tlakem (Ps), srovnání mezi indexy tahu, experimentálním tlakem (Ps) a silou při praktickém vytažení. Tyto indexy tahu zahrnují zatěžovací energii (W), odlehčovací energii (W´), hysterezi (H) a tahovou linearitu (TL). Výsledky ukázaly, že hodnota síly při praktickém prodloužení (F_L) má významný vliv na vysvětlení experimentálního tlaku (Ps). Rovněž se dospělo k závěru, že indexy tahu (W, W´, H a TL) statisticky vykazují významnost (hodnota R^2 = střední až silná) pro sílu při praktickém a experimentálním tlaku. Část 2 se skládá z teoretického zkoumání kompresního tlaku pomocí techniky modelování a transformace Laplaceova zákona. Tato technika pomohla prozkoumat některé neznámé parametry, zejména deformovanou šířku (w_f), skutečné napětí (σ_T) / logaritmickou deformaci (ε_T) / skutečný modul (E_T). Pomocí těchto neznámých parametrů byl Laplaceův zákon přeměněn na dva nové matematické modely. Model 1 (T.Y.M) je založen na skutečném Youngově modulu a Model 2 (E.Y.M) je založen na inženýrském Youngově modulu a deformované šířce (w_f). Kromě toho výsledky odhalily, že transformované modely model 1 a model 2 a základní Laplaceův zákon se dobře přibližují experimentálnímu tlaku (Ps). Stávající modely byly také porovnány s experimentálním tlakem za účelem analýzy jejich účinnosti. Nově transformované modely byly také statisticky porovnány s původním Laplaceovým zákonem a ukázalo se, že nově vyvinuté modely mají silnou významnou aproximaci k základnímu Laplaceovu zákonu.

Klíčová slova: *Charakterizace tahu, kotníkové střihy, modelační technika, transformované Laplaceovy zákony, experimentální tlak, přiblížení k Laplaceovu zákonu*

Nomenclature

List of Symbols

A_o	Original cross-sectional area [mm^2]
A	Actual cross-sectional area [mm^2]
C_L	Circumference of the leg [mm]
C_S	Circumference of socks [mm]
d	Diameter of the leg [mm]
d_L	Arc length of circular strip [mm]
H	Hysteresis
E_E	Engineering modulus [N/mm^2]
E_T	True modulus [N/mm^2]
F_L	Radial force /Practical force of extension [N]
ℓ	Final length [mm]
ℓ_o	Original length [mm]
ln	Natural log
L	The total length of the circular strip [mm]
$\Delta\ell$	Extended length/change in length [mm]
P	Pressure exerted per unit area [kPa]
Ps	Experimental pressure [kPa]
P_E	Pressure concerning engineering modulus [kPa]
P_T	Pressure concerning true modulus [kPa]
R	Radius of the leg [mm]
T	Tension on the cylindrical wall [N/mm]
t	Thickness of compression socks [mm]
w_i	Initial/un-stretched width of circular strip [mm]
w_f	Deformed width of circular strip [mm]
W	Loading energy [mJ]
W´	Unloading energy [mJ]
X	X-axis
Y	Y-axis
ε_E	Engineering strain
θ	Degree angle
ε_T	True strain

σ_E	Engineering stress [kPa]
σ_T	True stress [kPa]
λ	Draw ratio

List of Abbreviations

CEN	Committee of European Standardization
CCL	Compression class level
E.Y.M	Engineering Young's modulus [kPa]
ECE	European colorfastness establishment
FEA	Finite element analysis
ISO	International standard organization
ICC	International compression committee
MST	Medical stocking tester
Model 2 (E.Y.M)	Model 2 based on engineering Young's modulus
Model 1 (T.Y.M)	Model 1 based on true Young's modulus
PA	Polyamide
PU	Polyurethane
RH%	Relative humidity percentage [%]
T.Y.M	True Young's modulus [kPa]
H	Hysteresis
LE	Loading energy
UE	Unloading energy
TL	Tensile linearity

Table of Contents

List of Figures

List of Tables

1. Introduction

Compression socks are a highly acclaimed textile garment for the pressure exertion on the lower part of the leg. It is used for the prophylaxis and treatment of venous disorders in the human lower extremities. Venous diseases range from minor asymptomatic incompetence of venous valves to chronic venous leg ulceration. To reduce and get rid of venous hyper-pressure, a technique of compression therapy is recommended [1]. Leg ulcers affect 1% of the population of developed countries and imparts significantly negative impact to the quality of life. According to the estimation of UK Healthcare Commision , leg ulcer care costs the NHS (National Health services) about £300-600 million annually. Insufficient or non-sustained compression therapy will be less effective than sufficient and sustained compression due to an impaired hemodynamic effect [2]

1.1. Compression pressure mechanism

Mechanism of action is the lowering of pressure exertion from the ankle to the calf portion of the leg as shown in figure 1. The pressure gradient propels blood flows upward toward the heart instead of refluxing downward to the foot or laterally into the superficial veins. The application of adequate graduated compression reduces the diameter of major veins, which increases the velocity and volume of blood flow as revealed in figure 2. [3].

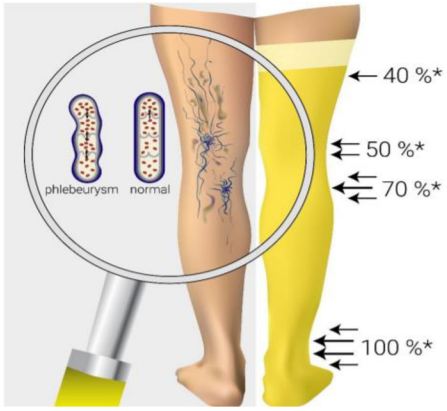

Figure 1. Mechanism of action of compression socks [4]

Figure 2. Comparison of reversible and irreversible blood flow [4]

1.2. Standard used for evaluation of compression socks

Various standards especially; British standard BS 6612:1985 [5], French standard ASQUAL [6], and German standard RAL-GZ 387/1:2000 [7] had been developed by different authorities in countries to describe the procedural requisites to evaluate and analyze the compression socks [8].

1.3. Classification of compression socks

Accoring to the European Committee for Standardization (CEN) and RAL-387/1:2000 [7], compression socks were classified to class I (2.4-2.8 kPa), class II (3.1-4.3 kPa), class III (4.5-6.1 kPa), and class IV (above 6.5 kPa). Class level also portrays the instensity of compression pressure at ankle (B portion). The extent of pressure (class level required) can be decided and recommended depending on the type and intensity of the disease. It includes to treat circulatory and vascular medical conditions as well as tired, sore, swollen, or aching legs [9],[10],[11],[12].

1.4. Principle of compression therapy

Medical compression socks with the gradual increase in compression pressure from distal to proximal regions are usually utilized to conduct the compression therapy. There are two main principles i.e. Laplace's law and Pascal's law, involved in explaining how the compression therapy system delivers the pressure around the leg. The first principle involves the application of Pascal's law, which demands muscle movement to generate a pressure pulse that is distributed evenly in lower limbs during active and passive exercise. Pascal's law is also used to explain the compression pressure during dynamic conditions. The compressive effect can reduce the diameter of veins by positioning valves and forcing the venous blood to return to the heart [13]. The second principle involves the application of Laplace's law to create a varied interface pressure based on limb shape as well as the tension of the stocking applied. This law is used to evaluate the compression pressure in static conditions [14].

1.5. Theory of Laplace's law

Using Laplace's formula, it is evident that the operative pressure should be greatest at the point of minimum girth area/radius and have the slightest pressure at the point of maximum girth area/radius. Thus, when compression socks are applied, the frontal feature of the leg encounters the highest amount of pressure while the lateral and medial sides of the leg receive the least compression pressure. Apart from the position of the leg, the circumference (thin or thick) of the

leg also needs optimum or lower pressure on cutaneous and subcutaneous skin layers which satisfies Laplace's law [15].

Based on the theory of Laplace's law that was developed to relate the wall tension and radius of cylinders (e.g. blood vessels) to the pressure difference due to inflation and deflation of two halves of cylindrical vessels [11],[16],[17]. The equation can be expressed as

$$P = \frac{T}{r} \tag{1}$$

where; P denotes pressure [Pa], T is the tension in the cylinder wall [N/m] and r is the radius of the cylinder [m].

This law is now widely used to explain and assess the pressure delivered to a limb of a known radius by a fabric under known tension..

1.6. How does Laplace's law work?

The law of Laplace explains the basic physiologic mechanisms involved in compression therapy. Figure 3 and equation 1 define that at constant tension and increasing radius (r2) being inversely proportional to the curvature of the wooden leg (flat curve) cause lowering of interface pressure (P1). While lower radius (r1) causes the higher value of the curvature cause the increase in interface pressure. It is well proven that sock's pressure can be calculated by analyzing the tensile behavior (modulus of elasticity). Higher the elasticity modulus, the lower will be the degree of extensibility. So modulus of elasticity and reduction percentage are main predictors of compression pressure [18].

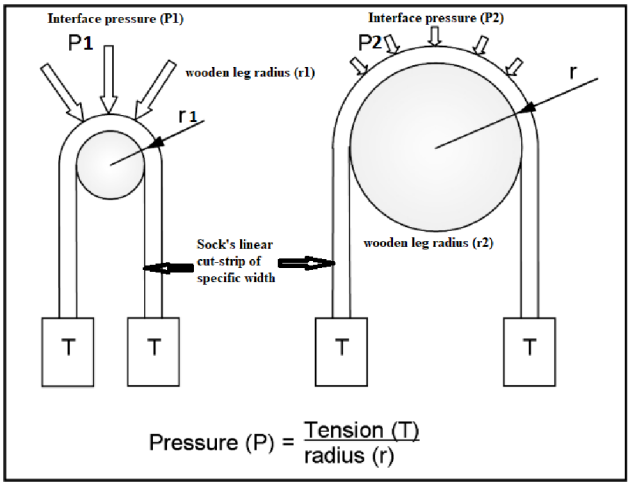

Figure 3. Theory of Laplace's law and mechanism of working

2. Purpose and the Aim of Study

The main purpose of current research was to investigate how well the tensile indices values explain the pressure results. It was also claimed to re-establish the pressure predicting mathematical models. For this modelization technique, there were introduced to transform basic Laplace's law by incorporating some new parameters. The main objectives of the current research are tabulated as follows;

Tensile characterization of compression sock's ankle cut-strips

- Force at practical extension compared to experimental pressure
- Comparison of hysteresis, force at practical extension and experimental pressure
- Comparison of loading energy, force at practical extension and experimental pressure
- Comparison of unloading energy, force at practical extension and experimental pressure
- Comparison of tensile linearity, force at practical extension and experimental pressure

Theoretical investigation to modify Laplace's law

- Development of model 1 considering true Young's modulus and deformed width (w_f); model 1 (T.Y.M)
- Development of model 2 considering engineering Young's modulus; model 2 (E.Y.M)

Statistical comparison of modified and existing models

- Experimental pressure compared to model 1 (T.Y.M) and Laplace's law
- Experimental pressure compared to model 2 (E.Y.M) and Laplace's law
- Experimental pressure compared to existing models
- Comparison of developed models and Laplace's law

3. Overview of the Current State of the Problem

a) The tensile properties of compression socks play a vital role defining periodical efficacy and targeted compression pressure. In the scientific literature, no research was found in which the combined influence of tensile indices (W, W′, H, TL), force at practical extension (F_L) and experimental pressure (Ps) has measured. Literaturely, a few studies exist in which tensile indices were relate to experimental pressure using Kawabata evaluation system (biaxial extension) [19],[20], [21], [22], [23], [24] instead of uniaxial tensile tester (followed in this study).

b) Many studies exist in which the theoretical prediction of compression pressure is done using a numerical approach; Finite-Element method (FE method) [25–34] and mathematical approaches by approximating/modifying the basic Laplace's law [35–49]. European Committee for Standardization (CEN) declared that the pressure values of compression garments are calculated by Laplace's law, where the tensile force is measured under semi-static conditions [35]. Equation of Laplace's law was applied on various objects; wooden legs [7], [19], [36-39], PVC cylinder [9], [40-42], biological vessels [43], wooden leg wrapped with neoprene fabric simulating the human skin morphology and then installed the socks [29], leg mannequin of varying anatomy of the leg and together on human leg as well wooden leg [12] ,[19],[44],[45],[47-49], to validate experimental compression pressure. Most of the researchers concluded that Laplace's law well explained the experimental pressure when worn onto wooden legs but there are a few researchers who disagree to this concept. Macintyre *et al.* (2004) concluded that Laplace's law predicted the pressure exerted by compression garments on a cylinder model with different curvature radii and Laplace's law significantly overestimated the compression pressure in some cases [11]. Costanzo and Brasseur (2013) proved the inadequacy of Laplace's law when applied to the biological vessel. This has a non-linear response to deformation that is difficult to measure because of the nonlinear hydrostatic response. To overcome this flaw of Laplace's law shear stress concept was introduced instead of hoop stress using multiple constitutive models [43],[46]. Liu *et al.* (2013) concluded that there existed considerable differences between the experimental and theoretic pressure values except for samples exhibiting more tuck stitches than others. Measured pressures in all specimens were considerably more than those predicted by Laplace's law. This difference

may be considered due to geometric and morphologic deformation in loops and stitches. [19]. In most of the above scientific research, the basic Laplace's law is used for the prediction of compression pressure but some of the researchers had claimed to modify it without any additional parameter except the notational changes which was the gap in this part of the research work. In this research work, it was introduced some missing parameters that can be incorporated for the modification of Laplace's law using the modelization technique. These unknown parameters include; true stress (σ_T), true/logarithm strain (ε_T), true modulus (E_T), engineering stress (σ_E)/ strain (ε_E) / engineering modulus (E_E) and deformed width (w_f). Using these mentioned parameters, two new models based on engineering Young's modulus and true Young's modulus abbreviated as Model 1 (E.Y.M) and Model 2 (T.Y.M) were developed. As per the literature review, none of the researchers has considered the viscoelastic behavior of the compression socks only justifying the theoretical and experimental difference is due to surface friction, stitches uneven deformation and slippage factor, etc. In real, compression socks being super-elastic when donned on the leg undergoes axial shrinkage after circumferential expansion causing the ultimate circumferential compression pressure.

4. Literature Review

4.1. Tensile characterization of compression socks

Compression garments are made of elastic materials hybridized with a combination of elastic and non-elastic materials. Extensibility and elastic recovery of compression garments are the most important operational characteristics because of which they can exert continuous pressure on the human body. During the wearing of compression garments, the hysteresis of fabric and dynamic elastic properties are also of great significance and affect the intensity and durability of compression stockings [50]. It is observed that there exist different modalities to be considered for the mechanical characterization of compression socks. It includes mainly elasticity, stiffness, hysteresis, pressure level, pressure delivery mode, materials, and fabrication technology [51],[52],[53].

The quality of compression capacity of socks depends on the characteristics of the materials used in manufacturing. All the materials for medical compression therapy have three major characteristics: i) elasticity; ability of the material to return to the original shape and size after stretching; ii) stiffness or elasticity coefficient; the increase in pressure after a certain given elongation. Here the stiffness depends on elasticity in static conditions; iii) hysteresis; the intuitive resistance of material as a result of internal friction hysteresis, that can be envisioned in a force/elongation curve. [54].

4.2. Modalities for tensile characterization

Three main characteristics comprehensively explain compression pressure depending on the type of pressure; static pressure or dynamic pressure. These three parameters are named; Elasticity, stiffness, and hysteresis

4.2.1. Elasticity

In elementary mechanics, the elasticity of spring is expressed by Hook's law which explains that the force necessary to stretch or compress a spring is proportional to how much it is stretched or compressed. In continuous elastic materials, Hook's law implies that stress is proportional to strain. Some materials such as rubber do not obey Hook's law except under very small deformation. Elasticity is the capacity of a material to return to its original shape when applied stretch or elongation is removed. The principle involved behind it can be explained by Hook's

Law (F=-k.x) where F (tensile force) is proportional to extension. Due to the presence of internal friction or plasticity, Hook's law is not obeyed and hysteresis (H) occurs when tensile loading is removed [53]. Liu *et al.* (2009) mentioned that the compression stockings of different elasticity (stretch) produced different skin pressure gradient (slopes) distribution, which significantly influenced the patient's venous hemodynamics (e.g., capillary filtration rate) [55]. Lim and Davies (2014) mentioned that the overall pressure is affected by the factors such as the elasticity and stiffness of stocking material, the size and shape of the wearer's legs, and the movements and activities of the wearer [56]. The proportion of stretch and force, which corresponds to the steepness of the so-called slope in the hysteresis curve, reflects the elasticity of the material of the stocking [57].

Rodica *et al.* (2010) studied the tensile and rheological features of compression socks by introducing Grab test method using Mesdan Tensolab. She proposed the Grab test method claiming as a real simulator for the durability assessment of compression socks. She concluded that the proposed testing method can be used to assess the graduated compression socks by measuring the deformation resulting in traction tests in three directions under two different levels. [58].

Wang *et al.* (2014) [59] and Lyle (1977) [60] studied dynamic pressure reduction of elastic fabric using a hemisphere-based pressure measuring device. Hemisphere pressure measuring devices sense static and dynamic pressure at predetermined press depths, velocities, and fixed test cycles imparting deformation. Thus, deformation produces pressure on the surface of the hemisphere. It was concluded that plain fabrics have higher dynamic pressure at all the extensions (10-40 %) that is reduced due to repeated extension (10-40 %) and recovery.

Liu *et al.* (2018) The stress-strain curves under the three cycles of loading were recorded to represent interactive relationships between tensile forces in Newtons and elongations (strain) of the tested specimens in percentage. The elastic moduli of the specimens were automatically recorded by the Instron testing system. The overall tension–stretch performances of the socks shells in horizontal (circumference) directions were determined, which dominate encircling pressures around the lower limbs [36].

Maklewska *et al.* (2006) [38], the values of force and relative elongation related to them were measured during the relaxation period of the fifth cycle (5^{th}) hysteresis loop for theoretical measurement of compression pressure (see equation 12).

Hui and Ng (2003) [61] theoretically analyzed the tension decay and pressure decay relating to the influence of spandex feeding rate and the fabric structure of the elastic fabric. The stress relaxation phenomenon was first observed by Ng [61], they found that all samples had relaxed their stress significantly, and the degree of stress-relaxation would also increase over time that a sample was under stretching.

Wang *et al.* (2011) [62] studied the elasticity and bursting strength of compression socks. Tensile properties of socks were measured in both wale and course directions. After fatigue stretching, the average immediate recovery of compression fabric is more than 95% and the average elastic recovery after an extended period of relaxation (1- 24 hours) is at least 98%. After 3 weeks of service and a few hours of relaxation, the compression fabric has only around 2% un-recovered elongation.

4.2.2. Stiffness

Partsch (2005) mentioned that The European pre-standard for compression hosiery (CEN) defines 'stiffness' as the pressure increase (in mmHg) per centimeter of circumference increase of the leg. This parameter is usually measured in the laboratory, but can also be assessed in the individual subject [63]. Stolk *et al.* (2004) have described a method to calculate a 'dynamic stiffness index' while walking [64]. Hirai *et al.* (2010) evaluated the reliability of a newly developed stiffness determining device by comparing the values with those obtained employing the Hohenstein method. They also introduced the concept of static stiffness and dynamic stiffness. The former is determined mainly based on laboratory testing using the Hohenstein method, while the latter is mainly measured by alterations in interface pressure during posture changes and exercise [65]. The dynamic stiffness index, like the stiffness index, is expressed in mmHg/cm. [53], [54], [64], [65], [66], [67], [68][69].

Partsch *et al.* (2007) [57] compared the interface pressure and stiffness properties of compression socks. They used sliced cut-strips and tested for stretch-tension curves using a Zwick dynamometer. In *vitro* method, static stiffness was calculated from the slope of the stretch/extension curve. It was concluded that interface pressure values are comparable with the

values calculated from the force/extension curves obtained using a dynamometer. Conclusion portrayed that correlation was highly significant between stiffness and compression pressure.

4.2.3. Hysteresis

Neumann (2013) mentioned that hysteresis is inborn resistance of material as a result of internal friction that can be visualized in the load-extension curve as shown in figure 4. By changing the speed of testing the angle toward the x-axis will move so the hysteresis is influenced by the speed of the movement. He mentioned that hysteresis is the most important parameter described by the difference between static pressure and dynamic pressure and researcher consider dynamic pressure rather than static pressure [54].

Wang *et al.* (2013) mentioned that apart from elasticity and recovery, the elastic fabric also shows a phenomenon of hysteresis, which is the stress relaxation of an elastic fabric after it has been subjected to repeated stretching and recovery. the elastic fabric has a characteristic of hysteresis which contributes to the pressure decay during wearing [59].

Ancutiene *et. al* (2017) investigated the tensile properties using the KES-F system [70]. The graphical representations of the stretch and recovery results portray the various mechanical properties of compression sock strips, directly and indirectly, influencing their pressure performance and long-lasting properties. The calculated tensile properties and definitions detained from the force-extension diagram are; loading energy [mJ], unloading energy [mJ], hysteresis, tensile linearity, and tensile practical stretch percentage [%], as shown in figure 4.

The property of hysteresis (H) could be a useful parameter to evaluate the viscoelastic properties of compression socks cut-strips. To obtain the areas bordered by the tensile and resilience curves, the trapezoidal rule was a simple and operative quadrature rule. The approximation of the definite integrals is referred to as the numerical integration or quadrature. According to the trapezoid rule, the partial sum of individual trapezoid areas could quantitatively present the hysteresis (H) when the fabric is stretched under a certain tensile loading as shown in figure 4.

Where H is the approximate area encircled by two load curves, $y1_i$ is the tensile curve (load increasing), and $y2_i$ is the resilience curve (load decreasing) [19].

The graphical representations (figure 4) of the stretch (1st cycle) and recovery (5th cycle) results portray the various mechanical properties of compression sock strips.

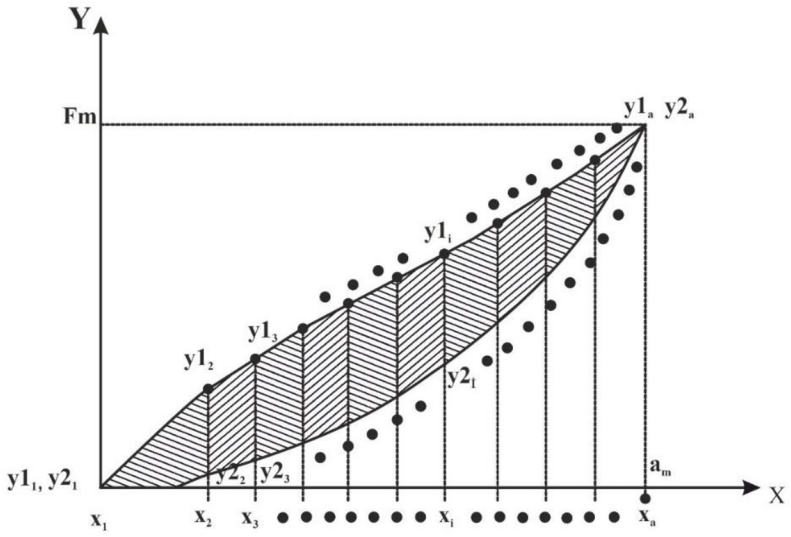

Figure 4. Load-extension curve [19]

The mathematical analysis was defined in the following way using equation 2.

$$H \approx \sum_{i=1}^{n-1} \frac{(y1_i - y2_i) + (y1_{i+1} - y2_{i+1})}{2}. \ (x_{i+1} - x_i) \qquad (2)$$

Loading energy

Tensile energy (W) is defined as the energy required for extending the fabric which reflects the ability of the fabric to withstand external stress during extension. The larger value of W associates a better tensile strength of the fabric [71]. It can also be defined as the area beneath the load-elongation curve [72], [73]. It can also be defined as 'The work done in stretching the fabric up to maximum deformation (a_m) is stored as potential energy or elastic strain energy [20]. Tensile energy was measured by plotting a pair of tensile force extension and recovery curves between zero and a maximum force as shown in figure 4. The tensile energy W can be quantitatively estimated by equation 3.

$$W = \int_0^x F(x).d(x) \qquad (3)$$

where; x is the displacement of the fabric stretched; F(x) is the tensile force needed in response to the stretched displacement [19].

Unloading energy

If the fabric undergoes a cycling loading process, the fabric is first stretched from zero stress to a maximum and the stress is fully released, then an unloading process follows the loading process. With the decreasing of the stretch loading, the return curve formed reflects the tensile resilience energy W' of the fabrics [19], which can be calculated by equation 4.

$$W' = \int_0^x F(x)'.\,d(x) \tag{4}$$

Tensile linearity

Tensile linearity indicates the wearing comfort. Lower values of the TL give higher fabric extensibility in an initial strain range indicating better comfort but the fabric dimensional stability decreases. Tensile linearity can be concluded as below

$$TL = \frac{2.W}{F_m.a_m} \tag{5}$$

where; F_m is the force at maximum deformation, a_m is maximum displacement, W is area under the loading curve [19]

Practical stretch and reduction ratio

It is the ratio of the circumferential difference between the leg and socks to the sock's circumference while reduction percentage is the ratio of the circumferential difference between the leg and socks to the leg's circumference calculated using equation 7 and equation 8. [7]

$$\text{Stretch ratio } (S_e) = \frac{L_c - S_c}{S_c} \tag{6}$$

$$\text{Reduction ratio } (R_e) = \frac{L_c - S_c}{L_c} \tag{7}$$

where; L_c is leg circumference, S_c is socks circumference

Liu *et al.* (2006) and Liu *et al.* (2018) evaluated the quantitative relationships between pressure and mechanical properties of stockings using the KAWABATA standard evaluation system (KES-FB). The results showed that compression stockings exhibiting different pressure is due to

significant differences in tensile, shear and bending properties (p value <0.001). In his both of researches, it was concluded that all these mechanical indices (W-tensile energy, EM-tensile strain, G-shear stiffness, and B-bending rigidity) significantly correlate with experimental compression pressure measured at the ankle and calf portion. It was statistically analyzed using multiple as well as logarithm regression equations [20],[22],[23].

Rong Liu *et al.* (2005) studied mechanical (tensile, bending, and shearing) and surface properties of different socks samples exhibiting varying physical properties using Kawabata Standard Evaluation System. They concluded that; Tensile indices like (W, W′) contributed strongly and revealed a strong co-relationship with compression pressure While, shearing (G, 2HG), bending (B) and weight (g/m^2) properties demonstrated medium but positive linear correlations with skin pressure gradient distribution [23].

Yamada and Matsuo (2009) [74] studied that stress-relaxation caused pressure degradation using the biaxial KAWABATA evaluation system. Studies have shown that the change in clothing pressure has been mainly based on its biaxial extension and stress-relaxation properties especially the value of the Hysteresis. Conclusively, it was found that the tensile load-strain curve provided much information to produce comfortable pressure garments. Also, the change in the curvature of an air pack was sensitive to the predicted clothing pressure value [74].

Ito *et al.* (1995) [75] studied the effect of biaxial stretch on compression pressure and concluded that it largely depended on its biaxial extension and stress relaxation properties.

Liu *et al.* (2013) designed 5 weft-knitted samples of varying tuck-miss-plain stitch combinations and three cycles of tension were set up between zero extension and the specified cycle load at 44 N when placing the fabric loop on the clamps. Tension curves to explore further their mechanical performance under tension includes; tensile energy (W), tensile resilience energy (W′), tensile linearity (TL), and hysteresis (H) [19].

4.3. Theoretical models developed and used for the prediction of pressure

As per the scientific literature review, it is observed that there exist the two most frequently used methodologies and techniques for the prediction of compression pressure include; Numerical modeling using the Finite element analysis technique (characterize the dynamic interaction between compression socks and human leg by simulating tools) and mathematical modeling

approach (characterize the static interaction between compression socks and solid leg/cylinder) by approximating the Laplace's law. [35-49]

In the European Committee for Standardization, pressure values of a compression garment are calculated by Laplace's law (equation 1), where the tensile force is measured under semi-static conditions [35], [73], [76].

German quality assurance standard (RAL-GZ 387/1) for the compression hosiery proposed to measure the static compression pressure based on the theory and principle of basic Laplace's law as shown in equation 8 [7]. This mathematical model is only applicable for specific kind of compression pressure measuring device designed by Hohenstein institute.

$$P_i = \frac{20\ \pi\ F_i}{U_i} \tag{8}$$

where; P_i= Compression at measuring point i [kPa], F_i= Tensional force at measuring point i [N/cm], U_i= Leg circumference at measuring point i [cm], U_i= Stand for measuring points B to G and for measuring clamps 1 to 20

Ng and Hui (2001) [12] and Halfaoui *et al.* (2016) [47] developed a model to predict interfacial pressure exerted on a fabric tube. In this study, they formulate a theoretical model to predict interfacial pressure is generalized as

$$P = \frac{2\ \pi\ \varepsilon\ E_i\ h_i}{C} \tag{9}$$

where; E_i is the modulus of elasticity [N/mm^2], h_i is the thickness of fabric [mm], C is the circumference of cylindrical fabric [mm], ε is engineering strain.

Ng and Hui (2001) [44] proposed objective method of to predict interfacial pressure induced by compression garments on a particular curved surface of the human body as well as on the cylinder by introducing the concept of reduction ratio to predict the compression pressure given below .

$$P = \frac{2\ \pi\ R_e\ EI\ t}{C_{tube}\ (1 - R_e)} \tag{10}$$

where; EI is the modulus of elasticity [N/mm^2], R_e is the reduction ratio, C_{tube} is the circumference of the cylindrical tube and t is the thickness

Most of the researchers concluded that Laplace's law well explained the experimental pressure when worn onto wooden legs except Macintyre *et al.* (2004) [11]. She concluded that Laplace's law predicted the pressures exerted by compression garments on a cylinder model with different curvature radii and concluded that Laplace's law significantly overestimated the compression pressure in some cases [11].

$$P = \frac{6.283\ T}{C} \tag{11}$$

where; P denotes pressure [Pa], T is the tension in the cylinder wall [N/mm] and C is the circumference of the cylinder [mm].

Maklewska *et al.* (2006) [38] designed and modeled warp fabrics used for compression therapy based on the pre-set value of unit pressure. The procedure was based on the theory of basic Laplace's law and knitted fabric mechanical characteristics in the form of non-linear force compared to relative elongation. Ultimately modifying the basic Laplace's law to predict the pressure values (equation 12). The test results of equation 12 on new manufactured stockings indicated that there was a close affinity between estimated and measured pressure values. The model is based on the theory of Laplace's law without exhibiting any parametrical change.

$$P_i = \frac{2\,\pi\,F}{W\,G_1} \tag{12}$$

where; F = force [N] of strip, G_1=circumference [cm] of model wooden leg, W = width [cm] of cut-strip,P_i = pressure exerted by the knitted fabric

Liu *et al.* (2018) measured the compression pressure experimentally on the wooden leg (in vitro) and human female legs (in vivo) using the Pico press pressure measuring device and the theory of Laplace's law (theoretical model). In the vitro test, surface stiffness and radius of curvature of the leg were maintained as identical while in the vivo test, mounted the panels with higher elastic moduli (shorter stretch) at the anterior region and with lower elastic moduli (longer stretch) at the posterior side of a leg as a condition I and mounted the panel with lower elastic moduli at the anterior region and with higher elastic moduli at the posterior region as condition II. Conclusively, condition II is more suitable for reshaping the pressure distribution. It was also concluded that the traditional wooden leg model may cause the overestimation of pressure dosages [36].

Liu *et al.* (2013) [77], Choi *et al.* (2010) [39], Bera *et al.* (2014) [9], Macintyre *et al.* [11], Cieslak *et al.* (2007) [46] and Troynikov *et al.* (2010) [78] designed knitted fabrics stitched tubular shape and applied to wooden leg for the experimental, measurement of compression pressure using Salzmann MST MKIV pressure measure device. For theoretical measurement of compression pressure basic equation of Laplace's law was used as mentioned in equation 1.

Dubuis *et. al.* (2014) [49] studied the patient-specific FE model leg under elastic compression and design a model to evaluate compression pressure. They established a theoretical model given below

$$P = \frac{\text{stiff } \varepsilon}{r} \tag{13}$$

where; stiff is the stiffness of the sock [N/mm], r is the curvature radius of the leg [mm], and ε is the strain of the sock in the horizontal plane. The latter was derived knowing leg and sock perimeters from the CT-scans.

Leung *et. al* (2010) [48] designed a new mathematical model (equation 14) for the prediction of compression pressure based on the theory of Laplace's law exerted by knitted fabrics (single layer and laminated fabrics). To design their model, they incorporated body circumference, original cross-sectional area, applied strain as a function of circumferential difference, and Young's modulus values. The correlation between Young's modulus and elongation were determined by analyzing the elongation behavior of samples. The results indicated that single-layer fabrics created a 34.6% deviation from actual test results. Meanwhile, the laminated fabrics created a 2.89% deviation from the actual results.

$$P = \frac{2\,\pi\,E\,A_o\,\varepsilon}{\ell_o(1+\varepsilon)\,C} \tag{14}$$

where; E is the modulus of elasticity [N/mm^2], C is the body circumference [mm], A_o is the original cross-sectional area of fabric [mm^2], and ε applied strain is a function of the circumferential difference between socks and leg.

Jariyapunya *et al.* (2018) developed knitted fabrics for the estimation of strain value. In this study, stress-strain curve data after the 5th cycle were used for the theoretical prediction modified based on the theory of basic Laplace's law thin-wall cylindrical theory as given in equation 15 [40].

$$P = \frac{2\,\pi\,\sigma_E\,d}{C} \tag{15}$$

where; σ_E is fabric circumferential stress [Pa], d is the thickness of fabric, C is the circumference of the cylinder

Zhang's *et al.* (2019) [42] used the concept of cylinder stress law with thin-walled assumption to design mathematical models for the prediction of compression pressure where the pressure P_i exerted by part i can be expressed as follows below

$$P_i = \frac{D_i\,E_i\,\ t}{r_{w.i}} \tag{16}$$

where; t is the thickness of cylinder, $r_{w.i}$ is the radius of part i of the cylinder while $N_{\theta.i}$ is the circumferential stress $N_{\theta.i}$, E is the tensile modulus and is calculated by using the equation $\Delta\sigma/\Delta\varepsilon$ where σ is the stress and ε is the strain, D_i is the axial length of the cylinder

Teyeme *et al.* (2021) modified the Laplace's law based on the theory of modelization by incorporating the parameters of engineering stress and strain values. The tensile test data obtained from Instron based on EN 14704-1 was incorporated into equation of Laplace's law (equation 1). Experimental pressure was measured by donning the stitched warp-knit fabric samples onto a PVC tube using a Pico press pressure device. Conclusively, theoretical results obtained with this modified Laplace's law compared to experimental pressure value were sufficiently good for use in compression garment design. Moreover, to verify the validity of the proposed model, experimental and predicted data were compared and very low error values were found [41].

$$P = \frac{E\,\varepsilon\,s\,2\pi}{C} \tag{17}$$

where; P is surface pressure, E is the modulus of elasticity, ε is engineering strain and C is the circumference of the leg and s is the thickness of the strip

5. Experimental Work

5.1. Procurement of compression socks

A total of 13 commercially available socks samples were purchased exhibiting three different compression class levels (Class I, 2.40~2.80 kPa; class II, 3.06~ 4.27 kPa and class III, 4.53~ 6.13 kPa; where (1 kPa =7.500 mmHg) [7]. Class 1 socks samples are coded as A1, A2, and A3;

Class II as B1, B2, and B3 while class III as C1, C2, C3, C4, C5, C6, and C7. Most of the socks (11 samples) exhibited (1×1 laid-in plain Knit) shown in figure 5(b). While only 2 samples belonging to class I exhibit (1×1 laid-in- mesh knit) portrayed in figure 5(a) were confirmed after visual and unravelling analysis. Socks samples were tested on fix-sized standard wooden legs exhibiting 240 mm circumference around the ankle.

(a) 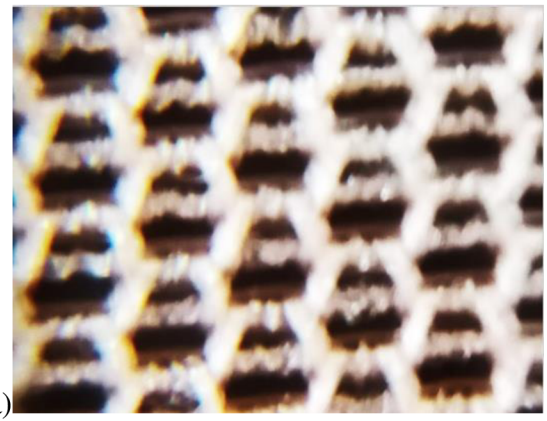 (b) 

Figure 5. (a) 1×1 laid-in- mesh knit (b) 1×1 laid-in plain knit

All of the samples were evaluated for their built-in physical and technical specifications as shown in table 1 and table 2 with great precision and accuracy under standard atmospheric conditions RH%, 65±5%, temperature, 20±2°C as per CEN 15831:2009 [35], and RAL-GZ 387/1 (Medical compression hosiery quality assurance) [7].

5.2. Preliminary testing of compression socks under study

Preliminary data of all 13 samples were evaluated at the ankle portion includes; fabric weight [g/m^2], fabric thickness [mm], quantitative analysis for polyurethane composition [%], type of yarns transformed to knit, stitch density, and circumference/width of the compression socks at ankle portion. All samples were categorized grounded on the 3-levels of compression classes (Class I, class II and class III) based on the intensity of compression pressure at the ankle mentioned in CEN 15831:2009 [35] and RAL-GZ 387/1 [7]. The class level is defined concerning pressure at the ankle portion because of being a complex part of the leg (contour and bony surfaces).

5.2.1. Determination of fiber content of the fabrics

Fiber analysis of all samples was done using the standard procedure mentioned in AATCC-20A-2013 and results are shown in table 1. To confirm the contents (polyamide/polyurethane) at the

ankle portion, there was marked a square of 50×50 mm² (250 mm^2) on both faces of compression socks as shown in figure 6(b), cut it to square form, unraveled the weft knitted threads to understand the yarn and knit type, as well as contents, etc. Unraveled threads were weighed for each sample seperately, and treated with an 95% solution of formic acid to dissolve the polyamide filaments as per the procedure mentioned in AATCC-20A method (Quantitative analysis of fiber composition), simultaneoulsy. The weight of the undissolved polyurethane extracted from all samples was done to find the percentage of polyurethane through the solubility test given in table 1 using the following equation.

$$\text{Polyurethane percentage } [\%] = \frac{\text{Weight of polyurethane threads}}{\text{Total weight of the threads}} . 100 \qquad (18)$$

Table 1. Physical specifications of compression socks

Sr. no.	Code	Circumference at ankle [cm]	Fiber analysis [%] *PU/*PA	Classification
1	A1	19.0	30/70	*CCLI (2.40–2.80 kPa)
2	A2	18.6	31/69	
3	A3	14.4	28/72	
4	B1	15.6	33/67	*CCLII (3.06–4.27 kPa)
5	B2	17.8	30/70	
6	B3	16.4	25/75	
7	C1	16.2	50/50	*CCLIII (4.53–6.13 kPa)
8	C2	15.6	45/55	
9	C3	14.6	38/62	
10	C4	17.8	28/72	
11	C5	15.6	40/60	
12	C6	14.6	32/68	
13	C7	16.2	45/55	

*PA=polyamide, *PU= polyurethane*CCL= Compression class level [7].

5.2.2. Determination of thread count of fabrics

The number of wales and courses per centimeter and stitch density per centimeter square were measured using the pick glass advised by the RAL GZ-387/1 standard of quality assurance [7].

Results of measured parameters; wales density (number of wales per cm), course density (number of courses per cm), and stitch density (stitches per centimeter square) are given in table 2.

5.2.3. Determination of thickness of the fabrics

Digital thickness tester of model M034A, SDL (Atlas) device was used to determine the thickness of the material according to standard test method ISO 5084:1996. The material is measured as the perpendicular distance between the base plate on which the fabric sample is positioned, and a circular pressing disc that develops on the surface of the fabric. The measurement progress is recorded by a computer program. The area of the pressing leg was 20cm^2 while the load of 200gram was applied. Thickness testing results are given in table 2.

5.2.4. Determination of weight per unit area of fabrics

Sample cut-strips; 250 mm^2 obtained from each sock were relaxed for 24 hours under controlled standard atmospheric conditions and were weighed using an electronic weighing balance. Given results in table 2 were calculated using the formula given below

$$\text{Fabric weight } \left[\frac{\text{g}}{\text{m}^2}\right] = \frac{\text{Average fabric weight } [\text{g}]}{\text{Area of fabric } [\text{cm}^2]} . 400 \qquad (19)$$

Table 2**.** Technical specifications of compression socks

Code	Thickness [mm]	Fabric Weight [g/m^2]	Course density [per cm]	Wales density [per cm]	Stitch density [stitches/ cm^2]
A1	0.40	139.44	22.4	19.21	430.43
A2	0.46	134.00	24.6	16.20	398.52
A3	0.54	149.28	18.20	20.00	360.00
B1	0.90	291.60	22.00	18.00	396.00
B2	0.75	298.00	22.60	18.27	412.90
B3	0.64	306.08	23.20	22.06	511.79
C1	0.69	281.60	20.80	22.41	466.12
C2	0.68	265.20	21.80	20.34	443.41
C3	0.65	296.00	21.00	23.44	492.24
C4	0.86	360.56	19.20	19.00	364.80
C5	0.70	298.44	24.00	22.00	528.00

C6	0.87	312.80	16.80	24.48	411.26
C7	0.72	384.88	22.60	26.00	587.60

5.3. Hand washing

Hand washing and rinsing of pair of each sock's samples was preceded before testing the physical and technical specification under slightly hot water for washing at a temperature of about 37±3 ^{o}C as per detailed specifications given below in table 3. The procedure comprised of dipping socks in a bucket for 10-15 minutes then were dehydrated (Hydro-extraction) by placing them flatly between two layers of towels for 24 hours under standard atmospheric conditions (RH%, 65±5%, temperature, 20±2 ^{o}C) for fully drying purpose proposed by socks manufacturing brands.

Table 3. Hand washing parameters

Parameters	Dipping time	Water temperature	Samples weight	Water quantity
Hand washed	10-15 minutes	37±3 ^{o}C	250 g	5 liters

5.4. Marking and slicing of cut-strips (ankle portion)

Initially, a dried sock sample was put onto a wooden leg in such a way that socks samples are not fully stretched to wales direction (longitudinal direction), considering no creases on the surface/face of fabric drawn a mark of mean-dashed-line (-); figure 6(a) corresponding to main-grooved-line engraved on the face of the wooden leg; figure 6(e). After marking the mean-dashed line (-), socks were put-off and allowed to be relaxed for 24 hours. After 24 hours, a square of 50×50 mm (250 mm^2) was marked keeping the drawn dashed line (-) as the mean line of the square marked on the face of the fabric. This was done to overcome variation due to repeated measurement of compression pressure and to keep the wales and courses smooth and straight.

Putting on and off all the hand-washed socks samples was done 5 times keeping the mean of the marked square, figure 6(c), at the main grooved line around the leg, and pressure was measured using the Salzmann MST MKIV model. Such a method of marking can be proposed to avoid the variability and reliability of compression pressure results. After marking and pressure measurement, a circular strip having widths of almost 50 mm was sliced into loop-strips as shown in figure 6(d). The slicing can be made at any position of leg up to thighs and arms in un-stretched

form. The sliced loop strips of all 13 socks samples were donned to the leg to measure deformed width (w_f) as revealed in figure 6(d).

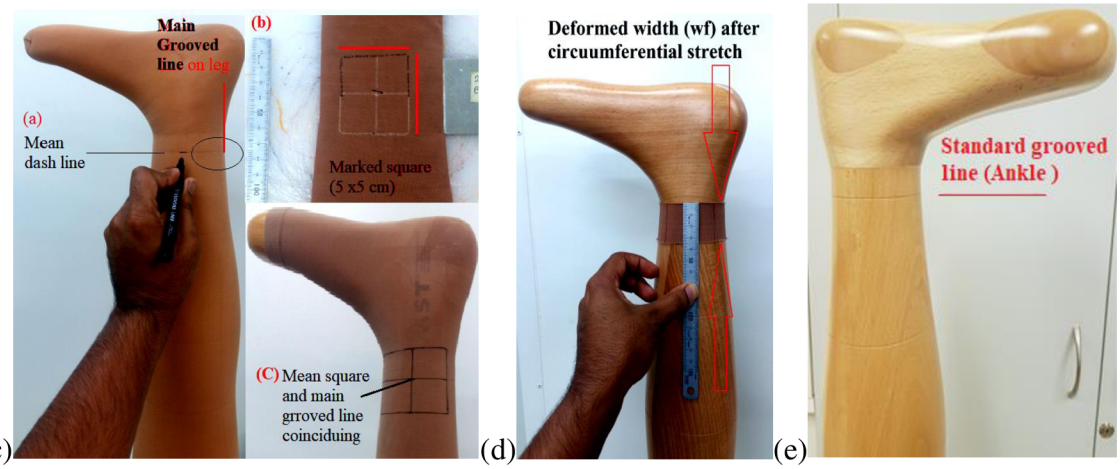

(a, b,c) (d) (e)

Figure 6. Marking (a) Locating exact grooved line on leg on the face of socks (b) Square marking 50×50 mm (250mm^2) (c) Coinciding mean line and main line over the sensor at the ankle on leg surface (d) Deformed width after wearing loop strip (e) Grooved line (ankle portion)

5.5. Wooden leg model

The compression pressure of each sock sample was measured on a standard-sized wooden leg arranged by Swisslastic standard leg producing company, located in Switzerland recommended by RAL-GZ 387/1 and CEN 15831. The circumference of the leg at ankle; cB = 240 mm while the length of the ankle from the sole of foot along the leg; ℓB = 120 mm (the height from the sole to grooved line on the face of leg at ankle portion) [7].

5.6. Measurement of experimental pressure

Currently, there are two major methods used for the determination of compression performance- the direct *in vivo* method and the indirect *in vitro* method using different tools. In this research work, we adopted *in vitro* method for indirect evaluation of compression pressure using the Salzmann pressure measuring device MST MKIV (Salzmann AG, St Gallen, Switzerland). This device is comprised of a thin plastic sleeve (4cm wide, 0.5mm thick), with four paired electrical contact points connected to an air pump and a pressure transducer. Sensors are located on the medial (inner) side of the wooden leg placed between the leg and socks as shown in figure 7. The air pump inflates the envelope until the contact open (when the inner pressure exerted by the air is just above external pressure due to the compression device). When the contact open, the

transducer reads the pressure at located measuring points and is displayed digitally with 0.15 kPa resolution. Two lengths of the probe are available. Only the shorter one (34cm long) with four contact points was used in this study. Such evaluation of compression measurement was performed under the standard test method RAL-GZ-387/1.

Figure 7. MST MKIV pressure measuring device

5.7. Force-extension curve analysis using the cut-strip method

In this scientific research, all the detached cut-strips were investigated for their tensile behavior. For this CRE (constant rate of extension) based Testometric tensile testing machine was selected and used.

5.7.1. Sample preparation

To investigate the tension behavior, all the circular cut-strips from the ankle part of compression socks were linearized into rectangular strips keeping the vertical edges of square mark of area 250 mm^2 between inner edges of clamps, alternatively as shown in figure 8(a). All 13 sample strips were allowed to be relaxed under controlled atmospheric conditions for 24 hours. Tensile testing along the wale direction is not tested here because there is no impact of the force of axial extension (longitudinal extension) on compression pressure. So decided to extend the cut-strips transversally to characterize the radial forces and measurement of tensile indices. Relaxed samples were cleaned by removing edging threads along the course direction to ensure inlaid threads must be griped to both clamping jaws to get an accurate and precise measurement of the force compared to extension data as publicized in figures 8(a) and 8(b).

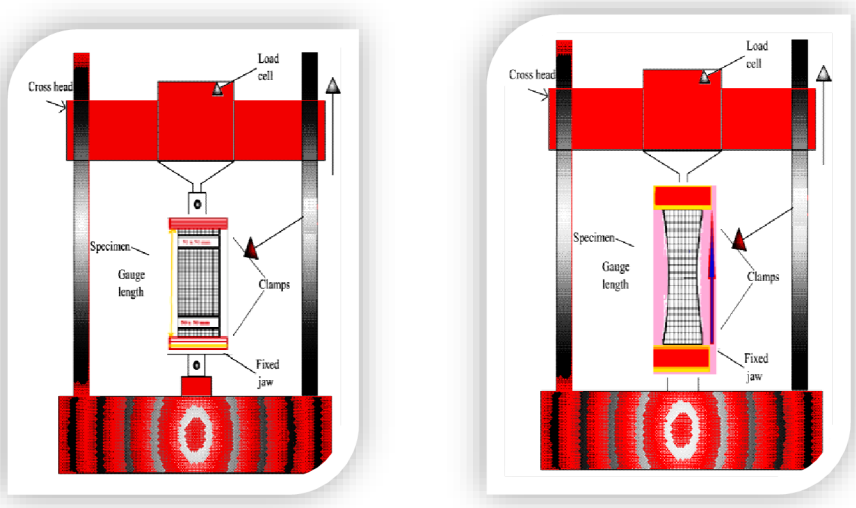

(a) (b)

Figure 8. (a) Clamped strip without extension, (b) Clamped strip after extension

The testing parameters and machine specifications were followed as per BS EN 14704-1 standard test method. Test specifications include: tensile rate, 100 mm/minute; specimen dimensions were 146~190mm×40~55mm (*lengthwise range of all cut-strips* × *widthwise range of all cut-strips*), gauge length adjusted was 50 mm. *Lengthwise range* means the strip lengths along the width of compression socks or in the course direction. While the *widthwise range* means the strip width along the length or the wales direction of compression socks.

Most of studies in which the strips are extended to fix extensions depending on the size of the object or requisite intensity of compression pressure. Ng and Hui (2001) [44] mentioned that elastic fabric is stretched in making up a pressure garment for clinical treatment generally ranges from 5-50%. While RAL-GZ 387/1 defines this range by mentioning that standard size hosiery can be a maximum of 50% of the extensibility transversely at all measuring points. Dongsheng *et al.* [80] proposed that clothing pressure increases linearly by increasing fabric elongation when it is within the 60% range. A person while wearing a tight garment transversal extension is not more than 60% the of initial length. Chattopadhyay *et al.* [81] mentioned during preliminary studies of pressure garments on several subjects that the maximum extension at which the samples were subjected during wear is about 60%. Therefore, it was decided to study the load elongation behavior of the test samples only up to 65% extension.

Due to these numerous reasons, it was understandable that the strips were extended transversally above 50% and below 70% literaturely. But the concept for the practical extension to predict compression pressure was never well-thought-out. Load-extension curve data of 5^{th} cycle at practical extension was used to characterize the tensile indices and influence of practical extension on force. This force at practical extension [mm] effect was also used for the prediction of compression pressure using developed mathematical models.

5.7.2. Cyclic-loading curve analysis

Five-times cyclic loading-unloading to all the cut-strips was performed between zero extensions to fixed extension (figure 9). Here figure 9 representing the first loading and 5^{th} unloading curve to characterize the tensile engineering of compression socks ankle cut-strips. Table 4 described physical specifications measured before and after testing. It includes; strip circumference (S_c); initial hoop strip width (w_i) before worn to wooden leg, deformed width (w_f) after worn to wooden leg shown in figure 6(d), thickness (t), original area (A_o) and force value at practical extension (F_L), experimental pressure (P_E) later used for the prediction of compression pressure using the theoretical modeling approach. A notational description of all parameters is described here. Gauge length/initial length/original length is denoted by 'ℓ_o', strips extended to practical elongation concerning gauge length (50 mm) are notated as '$\Delta\ell$' (extended length/change in original length) while the total length, 'ℓ' named as final or total length as the sum of gauge length and extended length ($\ell = \ell_o + \Delta\ell$). Where the difference between total length and gauge length was named extended length ($\Delta\ell = \ell - \ell_o$).

The tensile indices were measured by using only the 5^{th} cycle loading and 5^{th} cycle unloading curve's data at practical extension. These tensile indices include; loading energy (LE), unloading energy (UE), Hysteresis (H), and Tensile linearity (TL). Measured tensile indices were used to compare them with the experimental pressure values. Table 5 portrayed the tensile indices values extracted from the force at practical extension curve. These tensile indices using equations; hysteresis (equation 2), loading energy (equation 3), unloading energy (equation 4), tensile linearity (equation 6) was measured to compare their influence on the intensity of the compression pressure.

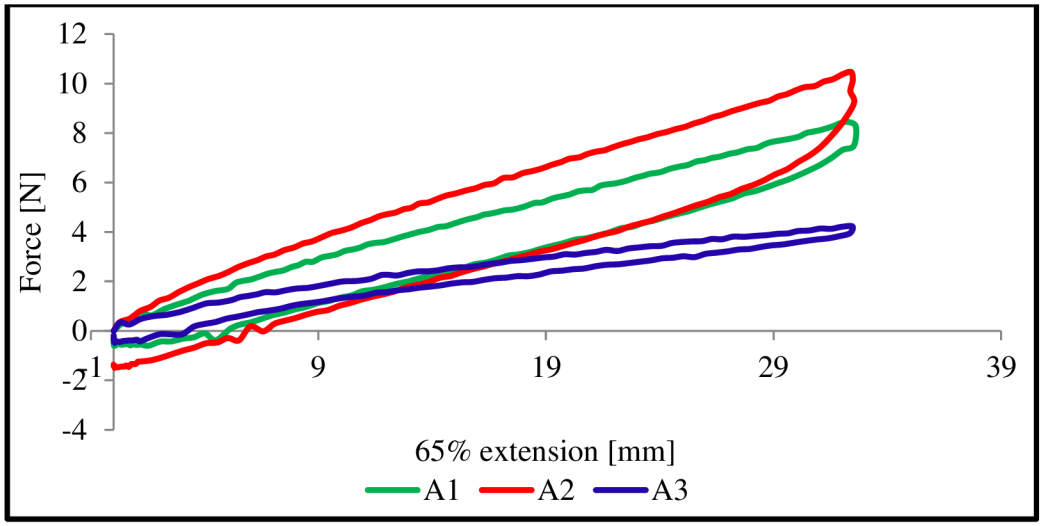

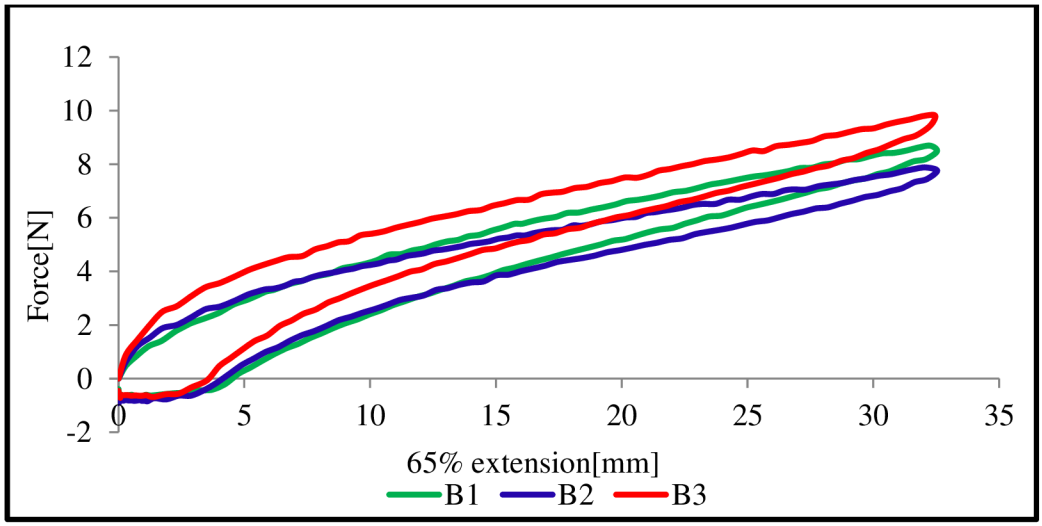

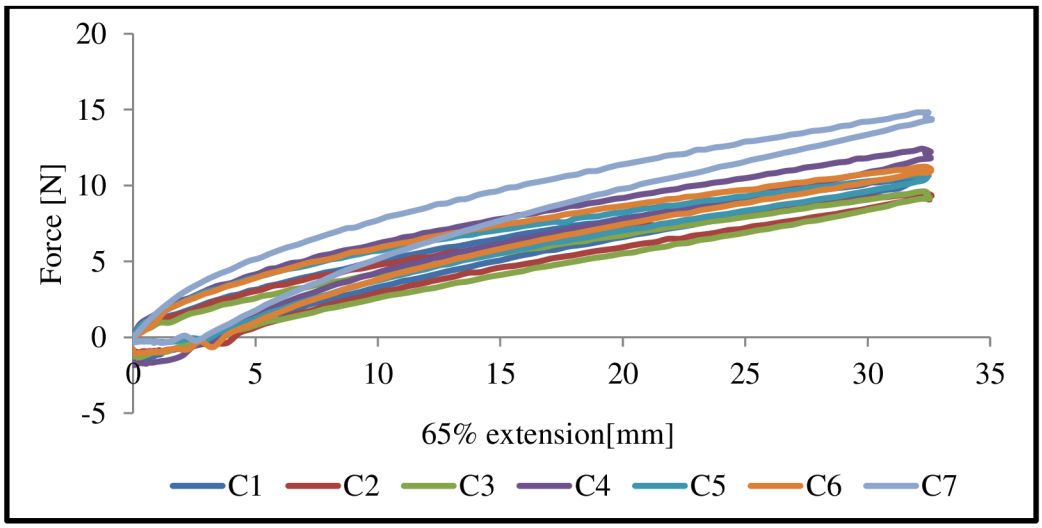

Figure 9. Force-extension curve at fixed extension (65%)

Table 4. Specifications of cut strips/compression socks/wooden leg

Code	Force at practical	Extended length	Initial width	Thickness	Deformed width	Original area	Final length	Socks circumference	Experimental pressure
	[N]	[mm]	[mm]	[mm]	[mm]	[mm^2]	[mm]	[mm]	[kPa]
	F_L	$\Delta\ell$	w_i	t	w_f	A_o	ℓ	S_c	Ps
A1	2.978	13.16	50.0	0.40	44.3	20.00	63.15	190	2.24
A2	3.416	14.52	46.5	0.46	43.0	21.39	64.51	186	2.4
A3	4.54	33.33	40.0	0.54	36.0	21.44	83.33	144	3.07
B1	7.872	26.92	54.0	0.90	48.0	48.65	76.92	156	3.65
B2	5.148	17.42	50.0	0.75	44.0	37.50	67.42	178	3.75
B3	7.72	23.17	54.0	0.64	48.0	34.56	73.17	164	4.34
C1	8.304	24.07	54.0	0.69	49.0	37.26	74.07	162	4.71
C2	8.238	26.92	48.0	0.68	42.0	32.64	76.92	156	4.83
C3	9.338	32.19	52.0	0.66	46.5	34.32	82.19	146	5.29
C4	7.928	17.42	50.0	0.86	45.0	43.00	67.42	178	5.33
C5	9.332	26.92	51.3	0.68	47.8	34.88	76.92	156	5.46
C6	10.972	32.19	50.0	0.87	45.0	43.50	82.19	146	6.26
C7	11.996	24.07	55.0	0.72	51.5	39.60	74.07	162	6.46

Table 5. Tensile indices values of compression socks' cut-strips

Code	Hysteresis	Loading energy [mJ]	Unloading energy [mJ]	Tensile linearity	Force at practical extension [N]
	H	W	W'	TL	F_L
A1	3.54	14.26	10.72	0.728	2.978
A2	4.36	16.16	11.8	0.652	3.416
A3	6.41	75.12	68.71	0.993	4.54
B1	12.96	103.78	90.82	0.979	7.872
B2	8.84	45.92	37.08	1.024	5.148

B3	19.77	107.24	87.47	1.199	7.72
C1	13.02	115.78	102.76	1.159	8.304
C2	13.42	116.29	102.87	1.049	8.238
C3	15.35	155.6	140.25	1.035	9.338
C4	11.78	71.96	60.18	1.042	7.928
C5	18.12	144.33	126.21	1.149	9.332
C6	14.671	199.421	184.75	1.129	10.972
C7	19.075	160.44	141.365	1.111	11.996

5.7.3. Loading curve at practical extension

Force at practical extension was extracted from the 5th cycle loading curve as shown below in figure 10. The practical elongation (equation 6) is calculated by considering the circumferences of the leg as well as of socks at the ankle portion. Here the circumference of the leg is fixed to 240 mm but each socks sample exhibit different circumferences at the ankle so the force of extension at specific practical elongation (extension level) is different. Figure 10 revealed the intensity of force of practical extension for all socks samples is different because of the varying parametrical and dimensional specifications.

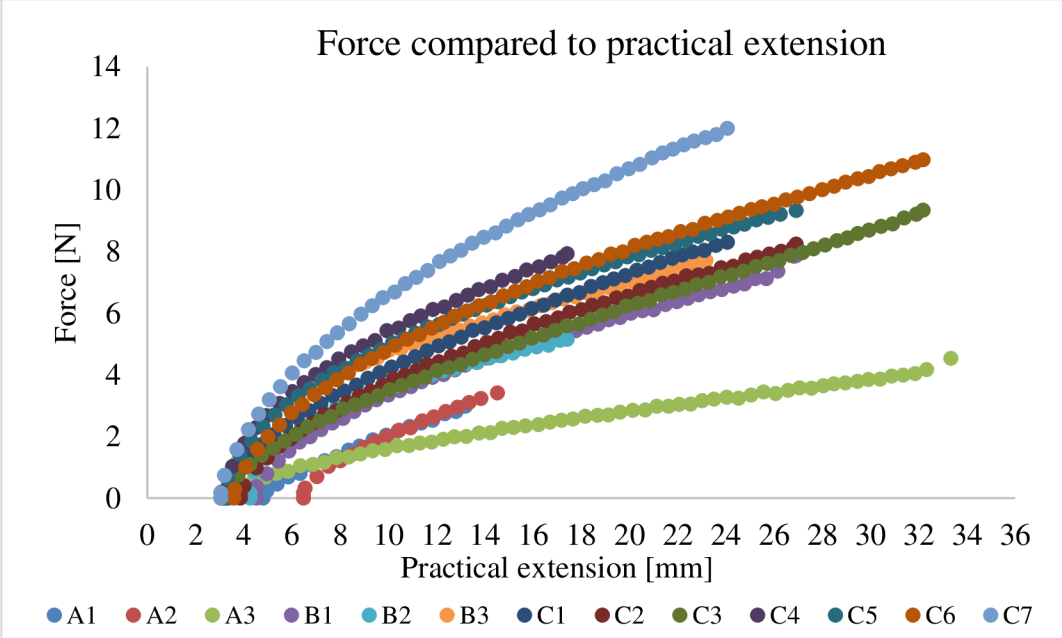

Figure 10. Force extension diagram at practical extension

5.8. Statistical analysis

All of the testing results were statistically analyzed using simple regression analysis. Regression analysis is the statistical tool used to define the data point's distribution by using the least-squares estimation method which derives the regression equation by minimizing the sum of the square of errors. The best-fit line is actually the regression model line. This regression line passing through data points gives us a regression model that helps to determine how well the independent variable explains the dependent variable. Regression results help to identify the direction, size, and statistical significance of the relationship between a predictors and responses. Regression equation provides 'best' fit line to examine how the response variable is changed by changing the predictor value as well as to predict the value of the response variable for any predictor value. The tools used in this research are coefficient of determination value (R^2-value) and Pearson correlation coefficient.

6. Modelling part

6.1. Modelization technique to analyze Laplace's law

The compression pressure (P) is defined by the force (F) which is exerted on an area of 1 m^2. From figure 11(a), the curvature of the leg plays a deciding role to quantify the extent of pressure on the surface of the human leg. This is described by Laplace's law stating that the pressure (P) is directly proportional to the tension (T) of compression socks but inversely proportional to the radius (R) of the curvature to which it is applied (see equation 1). Costanzo *et al.* [60] estimated the hoop stress in biological vessels using Laplace's law mentioning that commonly wall stiffness is measured by interpreting the slope of total hoop stress against strain as an elastic modulus but he used the mathematical Laplace's law model to estimate the hoop stress.

For prediction of compression pressure exerted by the circular strip, the circular strip was worn to the ankle portion of the wooden leg as revealed in figure 11(a). To evaluate the intensity of compression pressure on the surface of the wooden leg at the ankle portion, it was divided the circular wooden leg into two halves along with a deformed circular-cut strip as shown in figure 11(b). Each half portion of the circular cut strip when stretched and deformed width was analyzed and assigned the different notations describing the suppression of the cut-strip from the inner side.

Figure 12 is describing the mechanism of the force of exertion from the internal side of circular stretched cut strips per unit area of small arc length (dL= R. dθ) by the leg and the reversal force of exertion assumed to be interface compression pressure (P). To calculate the interface pressure (P) it was assumed the following limitations of the current model.

- Geometry of cylinder is axisymmetric
- Material is isotropic
- An axial force is assumed to be zero
- Friction between socks and leg is neglected
- Practical force (F_L) is assumed to be acting radially to exert interface pressure (P).
- The thickness of the circular cut strip after stretching is very small so assumed to be unchanged.
- Different stretch ratio as causing a decrease in the width of the circular cut strip as revealed in figure 11(a) is considered as deformed width (w_f)

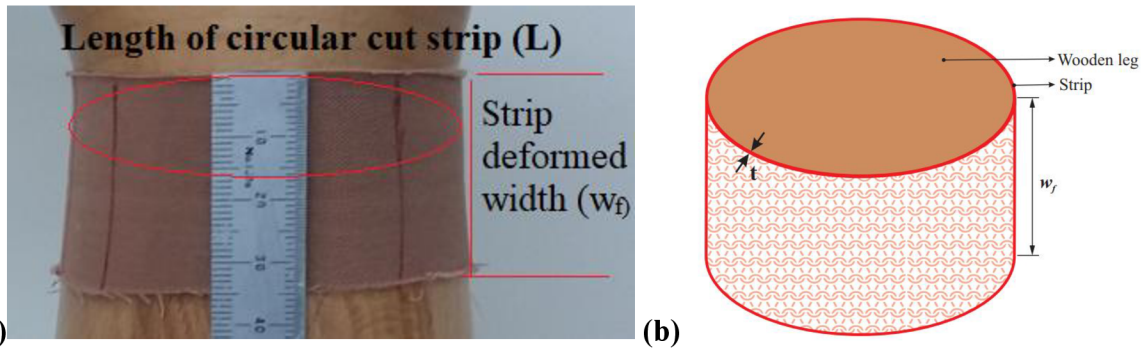

Figure 11. (a) Front view of the leg and cut-strip (b) Top view of cut strip worn to wooden leg

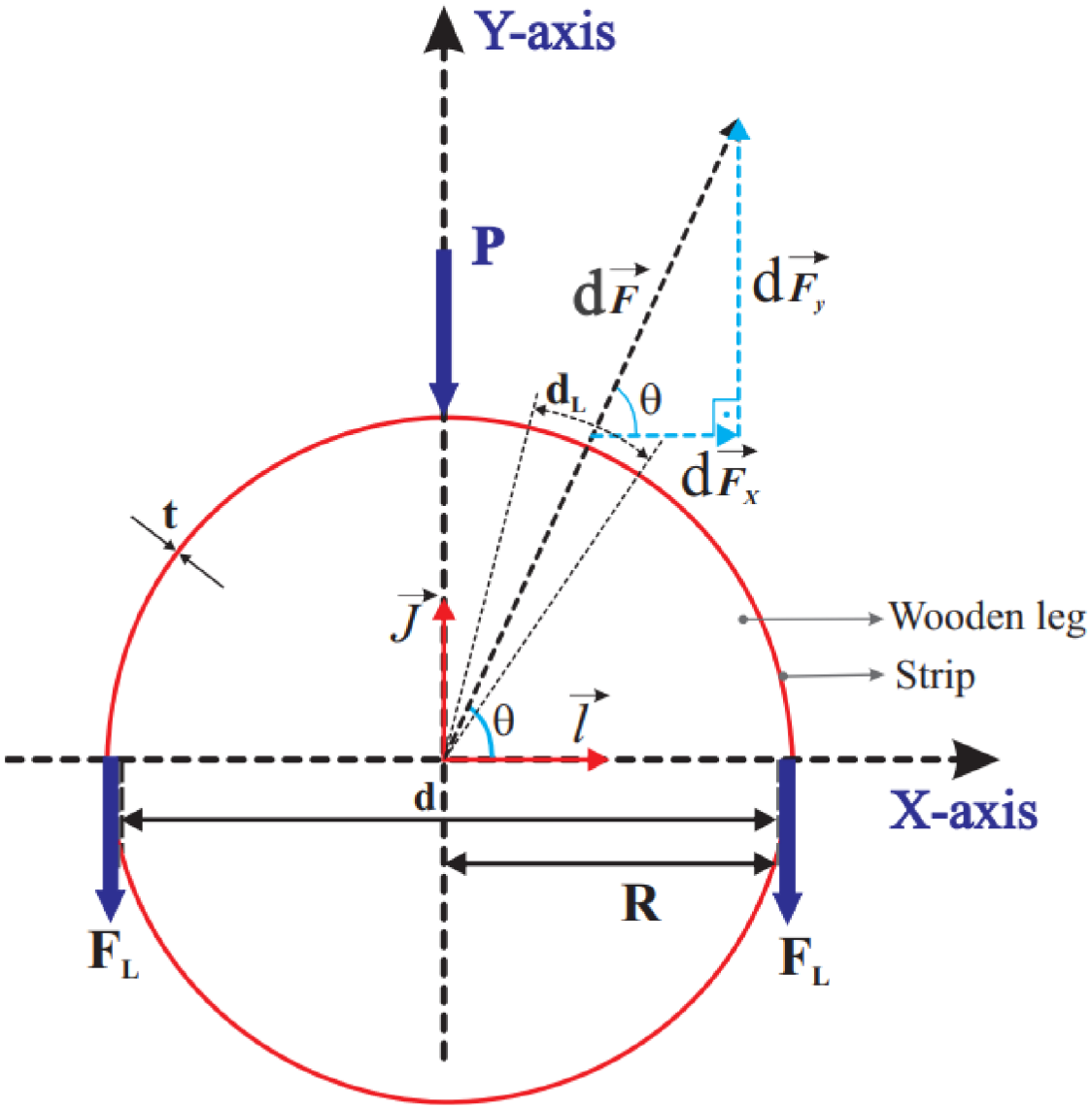

Figure 12. Mechanism of suppression of circular cut-strip due to the wooden leg

Laplace's law is the basic principle that attributes to characterize the graduated nature of compression hosiery. It describes the tension produced by a pressure gradient acting across the wall of an elastic cylinder. Laplace's law can be easily derived by considering the case for a static equilibrium where the force caused by the internal pressure (P) induced by a medium of width (w_i) stretched on a cylinder by a force (F_L) as publicized in figure 12. It was found that pressure exerted by a strip on the surface of the human leg has compatibility with Laplace's law.

F_L= Radial practical force [N]

d= Diameter of stretched socks/wooden leg [mm]

w_i= Initial width of circular strip [mm]

w_f= Deformed width of circular strip [mm]

L= Total length of strip [mm]

t= Thickness of compression socks [mm]

R= Radius of wooden leg [mm]

X= X-axis

Y= Y-axis/direction of pressure

d_L= Arc length of the circular strip [mm]

θ = Degree angle

P= Pressure exerted per unit area [kPa]

Due to static equilibrium condition

$$\sum \overrightarrow{F_y} = \vec{0}$$

The total sum of forces will become

$$2\vec{F} = \int_0^{\pi} \overrightarrow{P}\, w_f\, R\, d\theta$$

Where $\vec{P}$ can be replaced by $P.\sin\theta$ so the above equation will become

$$2F_L = P\, R\, w_f \int_0^{\pi} \mathrm{Sin}\theta.\, d\theta = P\, R\, w_f\, .(-1)[\cos 180° - \cos 0°]$$

$$2F_L = P\, R\, w_f\, [1 + 1] = 2\, P\, R\, w_f$$

$$F_L = P\, R\, w_f \qquad (20)$$

where; F_L is the radial practical force of cut-strip around the leg [N], P is radial pressure [kPa], R is radius of wooden leg [mm], w_f= deformed width [mm] of socks strip around the leg [41],[47], [48], [62],[82],[83],[84].

6.2. Development of model 2 (E.Y.M) in view of engineering Young's modulus

6.2.1. Engineering stress

The engineering measures of stress and strain notated in this research as σ_E are determined using the original specimen cross-sectional area A_0. Force and extension data were obtained using a Testometric tensile testing device. The corresponding engineering stresses and strains were calculated using equations 21 and 22.

Stress (σ) is defined as the force per unit area of a material so engineering stress can be calculated as

$$\sigma_E = \frac{F_L}{A_0} = \frac{F_L}{t\, w_i} \tag{21}$$

F_L = Tensile force applied to fabric [N], A_0 =Original cross-sectional area of the fabric [mm^2], t = Thickness of fabric [mm], w_i = Width of fabric [mm] [85].

6.2.2. Engineering strain

In terms of cut strips, strain (ε_E) is defined as extension per unit length so engineering strain can be defined and calculated using

$$\varepsilon_E = \frac{\text{Extended length}}{\text{Original length}} = \frac{\ell}{\ell_o} - 1 \tag{22}$$

Equation 22 can be used to measure stretch ratio/draw ratio (λ) which is the reciprocal of elastic coefficients

$$\text{Draw Ratio} = \frac{\ell}{\ell_o} = 1 + \varepsilon_E = \lambda \tag{23}$$

where; ε_E is engineering strain, ℓ is final length, ℓ_o is original length

In case of circular loop-strip and cylindrical wooden leg, the circumferential/longitudinal/practical strain is the ratio of circumferential difference between leg and socks to circumference of the socks using equation 6. Equation 22 and 24 shows the analogy between them.

$$\varepsilon_E = \frac{C_L - C_S}{C_S} = \frac{C_L}{C_S} - 1 \tag{24}$$

where; ε_E is engineering strain, C_L is the circumference of the leg, C_S is the circumference of circular socks strip [7],[85].

6.2.3. Measurement of deformed width

When the sock's circular-cut strips detached from the ankle portion were donned to the wooden leg at the ankle portion as revealed in figure 11(a) at practical elongation, the deformations in the strip's widths (w_f) were measured given in table 4.

6.2.4. Engineering modulus

Young's modulus, or the modulus of elasticity, is one of the most important measures of the mechanical properties of a material. However, it is difficult to obtain an exact stress-strain diagram on textile fibers even if we use the load-extension diagram as a substitute for the stress-strain

diagram. This is because the load-extension diagram does not make a straight line and because the percentage of extension is so high that many difficulties occur in determining Young's modulus. Generally, his modulus is measured while elongation is kept very small.

Here, ideally, elastic material (compression socks) satisfies Hook's law so, let σ_E be the engineering stress and ε_E be an engineering strain at any point in the straight-line region of the stress-strain diagram. Then, Young's modulus E is defined as the ratio of engineering stress to engineering strain so we can write

$$E_E = \frac{\text{Engineering stress}}{\text{Engineering strain}}$$

$$E_E = \frac{\sigma_E}{\varepsilon_E} = \frac{F_L}{A_0\,\varepsilon_E} \tag{25}$$

Here σ_E is engineering stress; ε_E is engineering strain while E_E is the modulus of elasticity [43],[46],[86],[87], [88],[89].

Comparing equation 20 and equation 25, we can get

$$F_L = F_L$$

$$P\,R\,w_f = E_E\,A_0\,\varepsilon_E$$

$$P_E = \frac{E_E\,A_0\,\varepsilon_E}{R\,w_i}$$

$$P_E = \frac{2\,\pi\,E_E\,A_0\,\varepsilon_E\,1000}{C\,w_i} \tag{26}$$

where; E_E is engineering elastic modulus [N/mm^2], w_f is deformed width of strip [mm], t is thickness [mm], ε_E is engineering strain, C is circumference [mm] and w_i is deformed width [mm], P_E is circumferential pressure exerted around the wooden leg [kPa]. Equation 26 is denoted as model 2 based on engineering Young's modulus (E.Y.M); model 2 (E.Y.M).

6.3. Development of model 1 (T.Y.M) in view of true Young's modulus

6.3.1. True stress

The stress is calculated based on the instantaneous area at any instant of load, and then it is the true stress. There could exist a relationship between the true stress and engineering stress once no volume change is assumed in the specimen. Under this assumption;

$$\text{True stress} = \frac{\text{Instantaneous load}}{\text{Instantaneous cross} - \text{sectional area}}$$

$$\sigma_T = \frac{F_L}{A} \tag{27}$$

where; A is the actual area of the cross-section corresponding to load F_L

Assuming material volume remains constant

$$A\,\ell = A_0 \ell_o$$

Based on the assumption of the above equation, equation 27 can be written as

$$\sigma_T = \frac{F_L\,A_o}{A\,A_0} = \frac{F_L\,\ell}{A_o\,\ell_o}$$

Using equations 21 and 23 in the above equation

$$\sigma_T = \sigma_E(1 + \varepsilon_E) \tag{28}$$

6.3.2. True/logarithm strain

True strain is defined as the instantaneous increase rate in the instantaneous gauge length defined as true strain [85],[90].

$$\varepsilon_T = \int_{\ell o}^{\ell} \frac{d\ell}{\ell}$$

$$\varepsilon_T = \ln(1 + \varepsilon_E) \tag{29}$$

6.3.3. True elastic modulus/Young's logarithm modulus

Using equations 28 and 29

$$E_T = \frac{\text{True stress}}{\text{True strain}} = \frac{\sigma_T}{\varepsilon_T}$$

$$E_T = \frac{\sigma_E(1 + \varepsilon_E)}{\ln(1 + \varepsilon_E)} \tag{30}$$

Equations 21 and 30 can be modified to

$$E_T \ln(1 + \varepsilon_E) = \frac{F_L(1 + \varepsilon_E)}{A_0}$$

$$F_L = \frac{E_T A_0 \ln(1 + \varepsilon_E)}{(1 + \varepsilon_E)} \tag{31}$$

Equating equations 20 and equation 31, relation will become

$$F_L = F_L$$

$$\frac{E_T\,A_0 \ln(1 + \varepsilon_E)}{(1 + \varepsilon_L)} = P\,R\,w_f$$

$$P_T = \frac{E_T\ A_0 \ln(1+\varepsilon_E)}{(1+\varepsilon_E)\ R\ w_f} \tag{32}$$

Equation 32 can be named Model 1 in view of true Young's modulus (T.Y.M)

As we know that the circumference of the leg (C) is C= 2πR so the radius can be calculated using

$$R = \frac{C}{2\pi}$$

Put the value of radius 'R' in equation 32, we can write

$$P_T = \frac{2\pi\ E_T\ A_0 \ln(1+\varepsilon_E)1000}{(1+\varepsilon_E)\ C\ w_f} \tag{33}$$

where; E_T is true engineering Young's elastic modulus [N/mm^2], w_f is deformed width of strip [mm], ε_E is engineering strain, C is circumference [mm] of the wooden leg at the ankle, w_f is deformed width [mm], P_T is circumferential pressure exerted around the wooden leg [kPa] based on the theory of true engineering Young's modulus. Equation 33 is denoted as Model 1 based on true engineering Young's modulus (T.Y.M); model 1 (T.Y.M).

Table 6 represents the theoretical measured values comprised of measurement of engineering stress (σ_E), circumferential/longitudinal/engineering strain (ε_E), engineering modulus (E_E) and deformed width (w_f), true stress (σ_T), true/logarithmic strain (ε_T), true elastic modulus (E_T) to be incorporated into modified mathematical models; model 1 (T.Y.M) mentioned as equation 33 and model 2 (E.Y.M) as equation 26. All additional supporting calculated parametrical values are also given in table 4 helped to measure the values given in table 6.

Table 6. Theoretical results of cut-strips for pressure predictions

Code	Engineering stress	Longitudinal engineering strain	Engineering modulus	Deformed width on leg	True stress	True strain	True modulus
	σ_E	ε_E	E_E	w_f	σ_T	ε_T	E_T
	[N/mm^2]	No unit	[N/mm^2]	[mm]	[N/mm^2]	No unit	[N/mm^2]
A1	0.149	0.263	0.566	44.3	0.188	0.234	0.805
A2	0.160	0.290	0.550	43.0	0.206	0.255	0.808

A3	0.210	0.667	0.315	36.0	0.350	0.511	0.686
B1	0.162	0.538	0.301	48.0	0.249	0.431	0.578
B2	0.137	0.348	0.394	44.0	0.185	0.299	0.619
B3	0.223	0.463	0.482	48.0	0.327	0.381	0.859
C1	0.223	0.481	0.463	49.0	0.330	0.393	0.840
C2	0.252	0.538	0.469	42.0	0.388	0.431	0.901
C3	0.272	0.644	0.423	46.5	0.447	0.497	0.900
C4	0.184	0.348	0.529	45.0	0.249	0.299	0.832
C5	0.268	0.538	0.497	47.8	0.412	0.431	0.955
C6	0.252	0.644	0.392	45.0	0.415	0.497	0.834
C7	0.303	0.481	0.629	51.5	0.449	0.393	1.142

7. Results and Discussion

In this scientific research work, the tensile properties of socks's cut strips were statistically compared with experimental pressure and force at practical extension. These tensile properties include; hysteresis (H), loading energy [mJ], unloading energy [mJ], and tensile linearity (TL). Secondly, theoretically developed models for the prediction of compression were also statistically equated with experimental pressure, existing models, and Laplace's law to estimate their mutual significance. To determine a relationship between any of two variables, Pearson correlations (r) and coefficient of determination values (R^2-value) were computed with a significant threshold set at $p < 0.05$.

7.1. Force at practical extension compared to experimental pressure

Figure 13 portrays the effect of force at practical extension on experimental pressure (Ps). The practical force of extension is the function of compression pressure exerted by the cut-strips. This function of exertion is defined mainly by Laplace's law and various researchers. The contribution of the force of the practical extension to compression pressure was statistically analyzed using simple linear regression analysis. Regression analysis is the statistical tool used to define the data point's distribution by using a best-fit regression line considering the minimum sum of the square of errors. This regression line passing through data points gives us a regression model that helps to determine how well the independent variable (force at practical extension) explains the dependent variable (experimental pressure).

Statistical results shown in figure 13 has revealed that force at practical extension imparts a significant influence on the intensity of compression pressure. It was quantified based on the coefficient of determination values (R^2 -value =0.9431). This R^2 -value depicts that the intensity of pressure exertion depends about 94.31% to the practical force of extension [N]. The regression model (figure 13) also comprised of the two more important coefficients explaining the nature and trend of the regression line. These regression coefficients are named y-intercept (0.8997) and slope value (0.4714). Here y-intercept value (0.8997) means the regression line intercepts the y-axis at 0.8997 which is very closer to the origin of axes while the slope gives the rate at which the dependent variable can be explained by the independent variable. The slope values (0.4714) also indicated that experimental pressure will increase by 0.4714 kPa for every increase in 1 unit

of force at practical extension. The correlation value between the force of practical extension and experimental pressure was also measured (r= 0.9603) which also shows a direct positive relationship between the two mentioned parameters. The reason for the dependency of the practical extension [mm] on compression pressure is mainly due to cut-strips areal density (fabric weight).

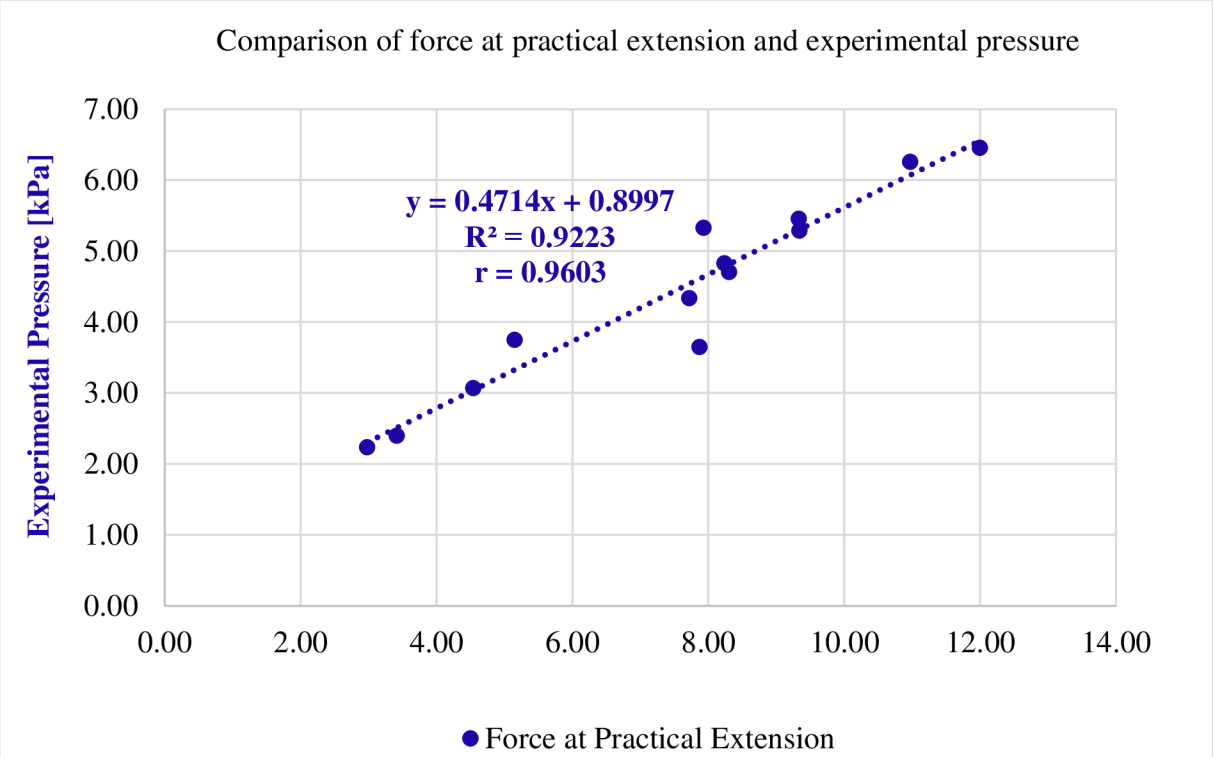

Figure 13. Force at practical extension compared to experimental pressure

7.2. Hysteresis

Figure 14 illustrates the relationship between force at practical extension (F_L), hysteresis (H) and experimental pressure (P_S). But it was necessary to relate how well the hysteresis (H) values of all socks samples explains the experimental pressure (Ps) and force at practical extension (F_L).

Figure 14 portrayed that hysteresis value of all the samples explain 74.7% to the experimental pressure values. The strength of the significance was measured on the basis of the coefficient of the determination values (R^2 value= 0.747) and correlation (r=0.864; strong positive Pearson correlation coefficient) using second order polynomial fitting line in regression analysis. It also portrayed that hysteresis has a very strong relationship with force at practical extension values.

The extent of dependency was computed based on the basis of coefficient of the determination value (R^2=0.8297) and direction of the relationship using Pearson correlation coefficient (r=0.910; strong positive correlation). This shows that hysteresis values of all samples explain the 82.97% to force at practical extension.

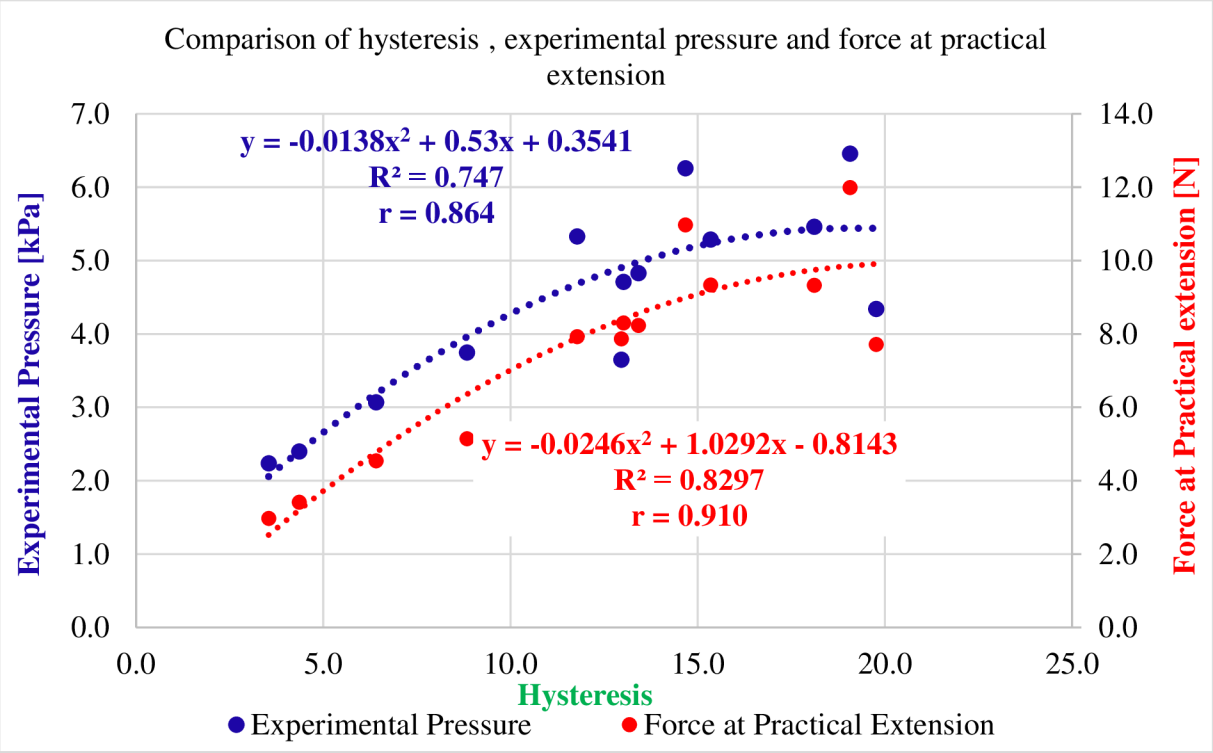

Figure 14. Hysteresis and force at practical extension compared to experimental pressure

7.3. Loading energy

Figure 15 represents the relationship between the force of practical extension (F_L), loading energy (LE), and experimental pressure (P_S). The extent of the dependency was measured on the basis of the coefficient of the determination values (R^2 -value) and Pearson correlation coefficient (r). As the loading energy increases, the area under the loading curve increases which increases the intensity of experimental pressure (Ps). The greater the tensile energy and tensile strain, the easier the fabric deforms in stretch loading [40].

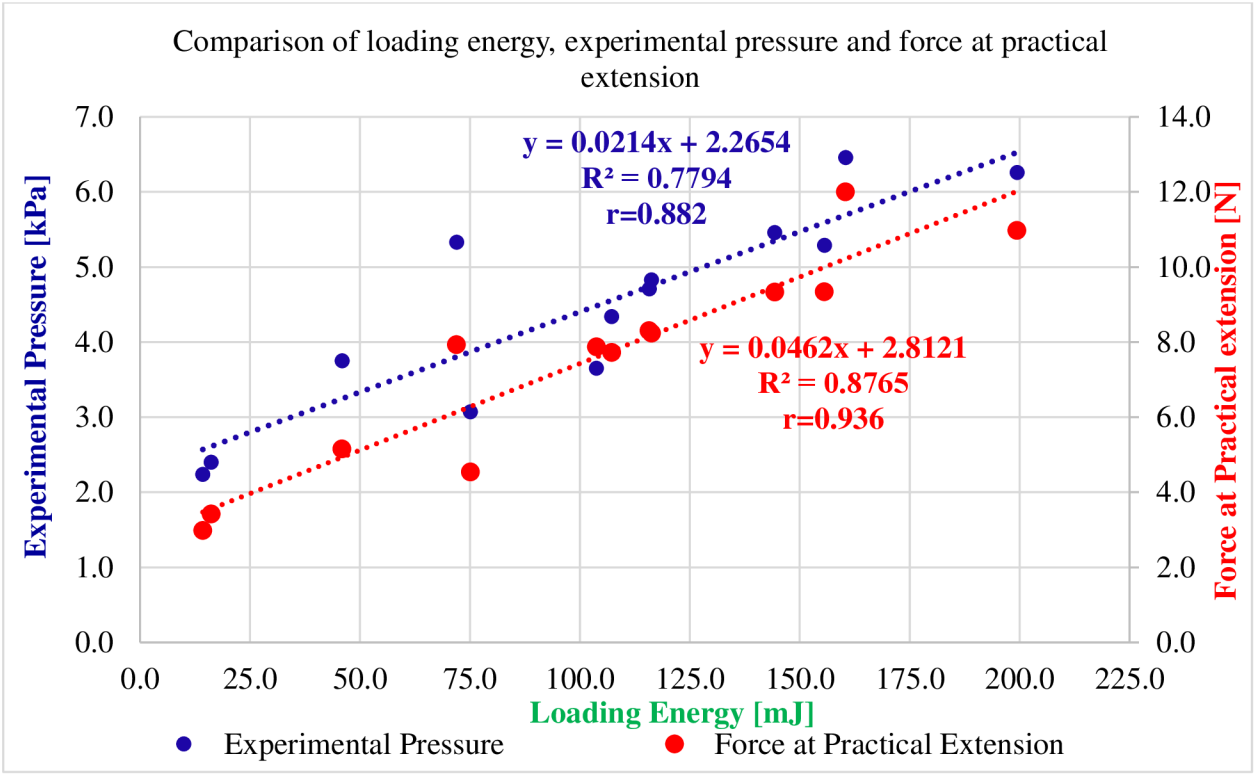

Figure 15. Loading energy and force at practical extension compared to experimental pressure

Higher deformation causes higher recovery of fabric to return to its original position ultimately increasing the intensity of compression pressure. The strength and direction of the relationship between loading energy (as predictor) and experimental pressure (response variable) was R^2=0.7794 and r=0.882. While extent of the relationship between loading energy and force at practical extension was R^2=0.8765 and r= 0.936. These R^2 and r values represents that loading energy explains the experimental pressure about 77.94% and correlation value r= 0.936 (strong positive relationship). While to the force at practical extension explains the loading energy about 87.65%.

7.4. Unloading energy

Figure 16 reflected the relationship between unloading energy (UE), force at practical extension (F_L) and experimental pressure (Ps) of all the 13 socks samples. Figure 16 also replicated that unloading energy (UE) has a direct relationship with the experimental pressure (Ps) which means as the unloading energy (UE) increases the compression pressure (P_S) value increases.

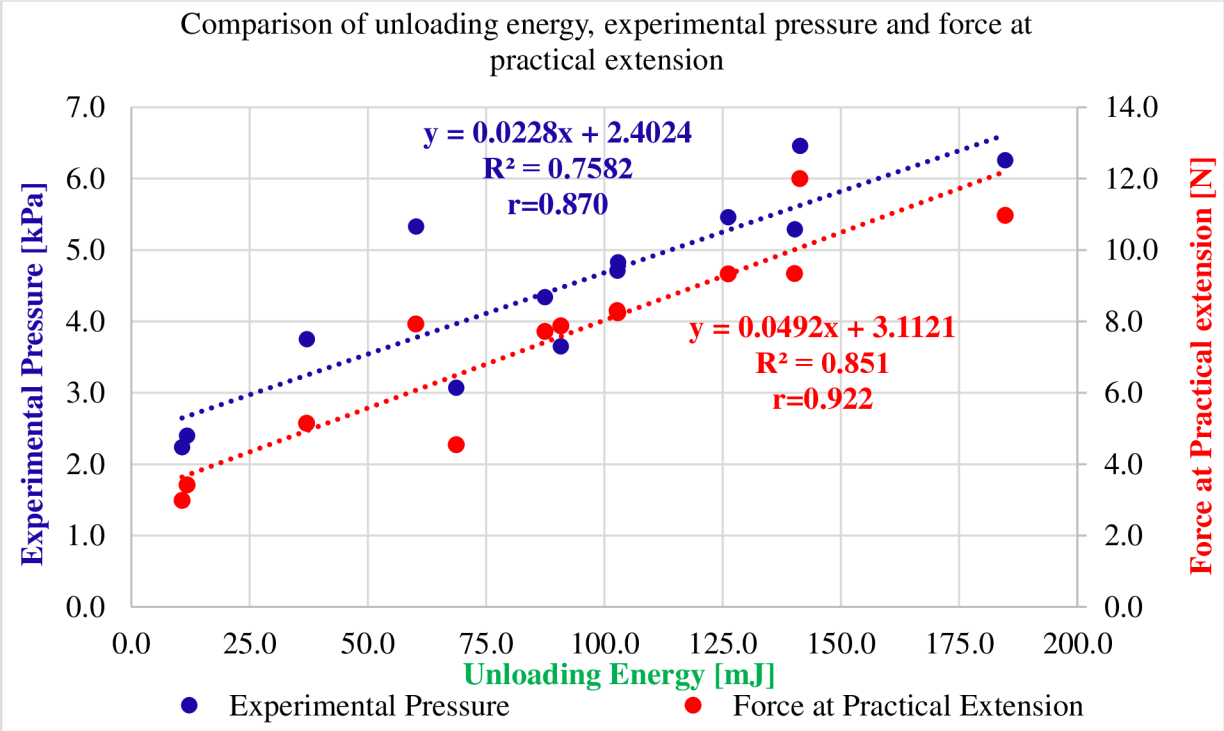

Figure 16. Unloading energy and force at practical extension compared to experimental pressure

Simple linear regression analysis was also conducted to observe the strength of the influence of the unloading energy (UE) to force at practical extension (R^2 -value =0.851and r= 0.922) and experimental pressure (R^2 -value =0.7582 and r=0.870) by measuring the coefficient of the determination value and correlation. These values portray that unloading energy (UE) explains experimental pressure about 75.82% and to force at practical extension 85.1% simultaneously.

7.5. Tensile linearity

Figure 17 comprised of the relationship between forces at practical extension, tensile linearity, and experimental pressure. To understand their mutual dependency, linear regression analysis was conducted to quantify it. Figure 17 portrays that the tensile linearity explains experimental pressure to 59.92% based on the coefficient of the determination values (R^2 -value = 0.5992, r= 0.773). While it explains to force at practical extension about 58.85% based on the coefficient of the determination values (R^2 -value = 0.5885, r= 0.7671).

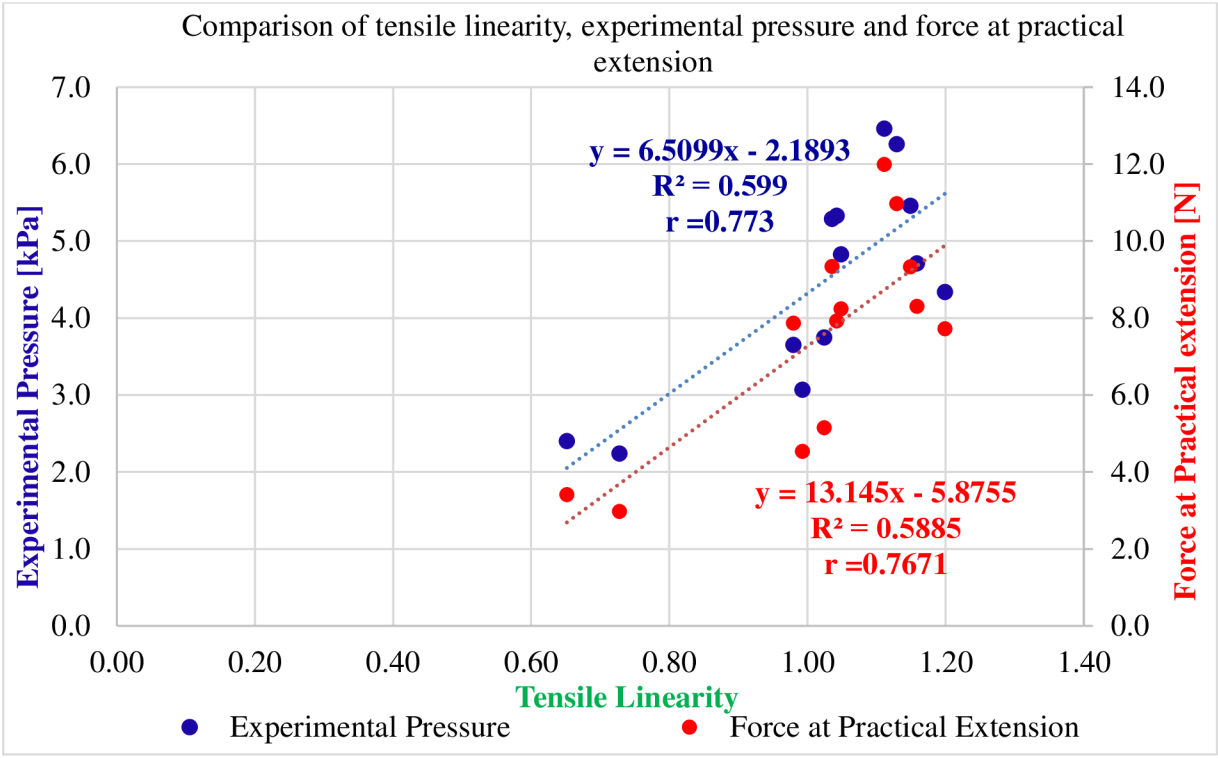

Figure 17. Tensile linearity and force at practical extension compared to experimental pressure

7.6. Statistical analysis between experimental pressure, modified models, and Laplace's law

7.6.1. Experimental pressure compared to Model 1 (T.Y.M) and Laplace's law

Figure 18 represents the relationship between experimental pressure (predictor) compared to model 1 (T.Y.M) and Laplace's law (responses).

Figure 18 represents the strength of the relationship between predictor; experimental pressure to response variables; model 1 (T.Y.M) based on the coefficient of determination value notated as R^2-value (0.9197). It means the newly transformed model; model 1 (T.Y.M) based on the theory of true Young's modulus explains 91.97% to experimental pressure results. In the regression model, there are two coefficients; coefficient of predictor (slope =0.9949) and constant (y-intercept = -0.137) defines the steepness of the line and the point at which the regression line connects the response variable (y-axis). Greater the magnitude of the slope, the steeper the line and the greater the rate of change.

Figure 18 also shows that relationship between original Laplace's law and experimental pressure was analyzed using simple linear regression analysis. The extent of the relationship was measured

based on the coefficient of determination value ($R^2 = 0.9319$). In the regression model, there are two coefficients; coefficient of predictor (slope =0.9216) and constant (y-intercept = -0.2296) defines the steepness of the line and the point at which the regression line connects the response variable (y-axis). Coefficient of determination values (R^2-value) of newly transformed model; model 1 (T.Y.M) is about 2% lower than original Laplace's law when was compared to experimental pressure.

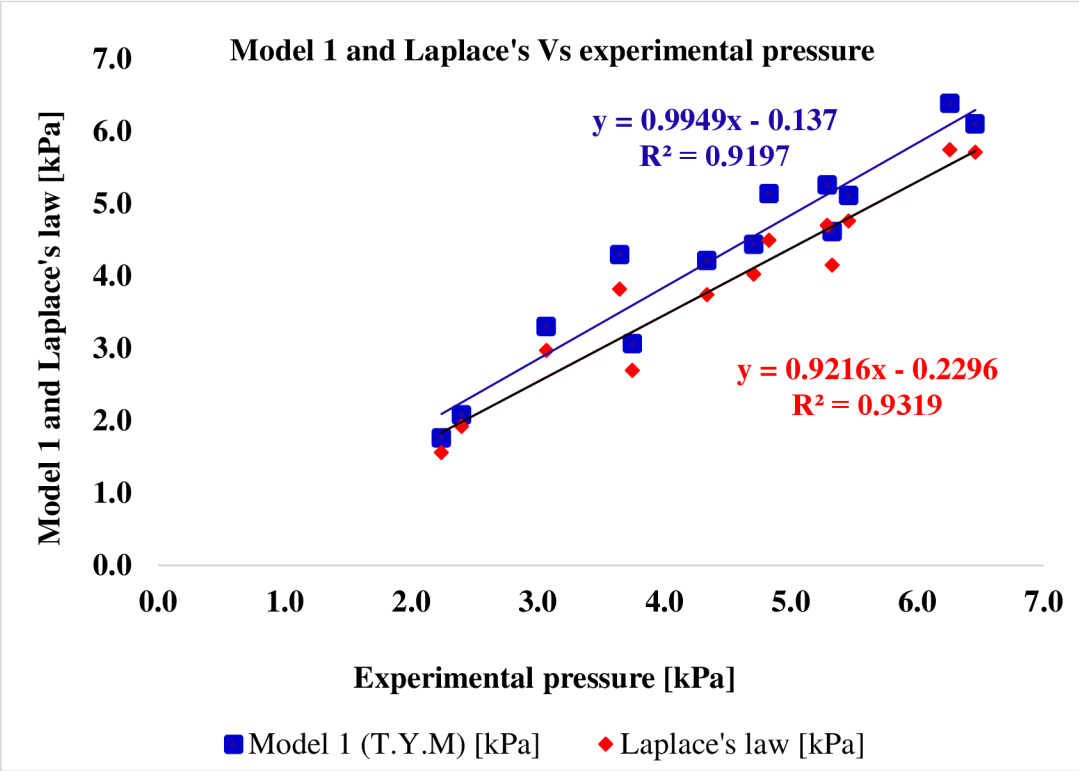

Figure 18. Experimental pressure compared to model 1 (T.Y.M) and Laplace's law

7.6.2. Experimental pressure compared to Model 2 (E.Y.M) and Laplace's law

Figure 19 portrays the relationship between predictors; experimental pressure compared to response variables; Model 2 (E.Y.M) and Laplace's law. The results based on the value of the coefficients (slope and y-intercept) helped to calculate the coefficient of determination values. Coefficient of determination values calculated between Laplace's law and transformed model; model 2 (E.Y.M) compared to experimental pressure was same ($R^2 = 0.9319$) except the slope and y-intercept values. R^2-value represents that both Laplace's law and transformed model 2 explains the 93.19% to experimental pressure results. The calculated compression pressure

measured using transformed model 2 and Laplace's Law are similar but in figure 20 for Laplace's law, experimental pressure is considered on y-axis to show the two different regression lines separately.

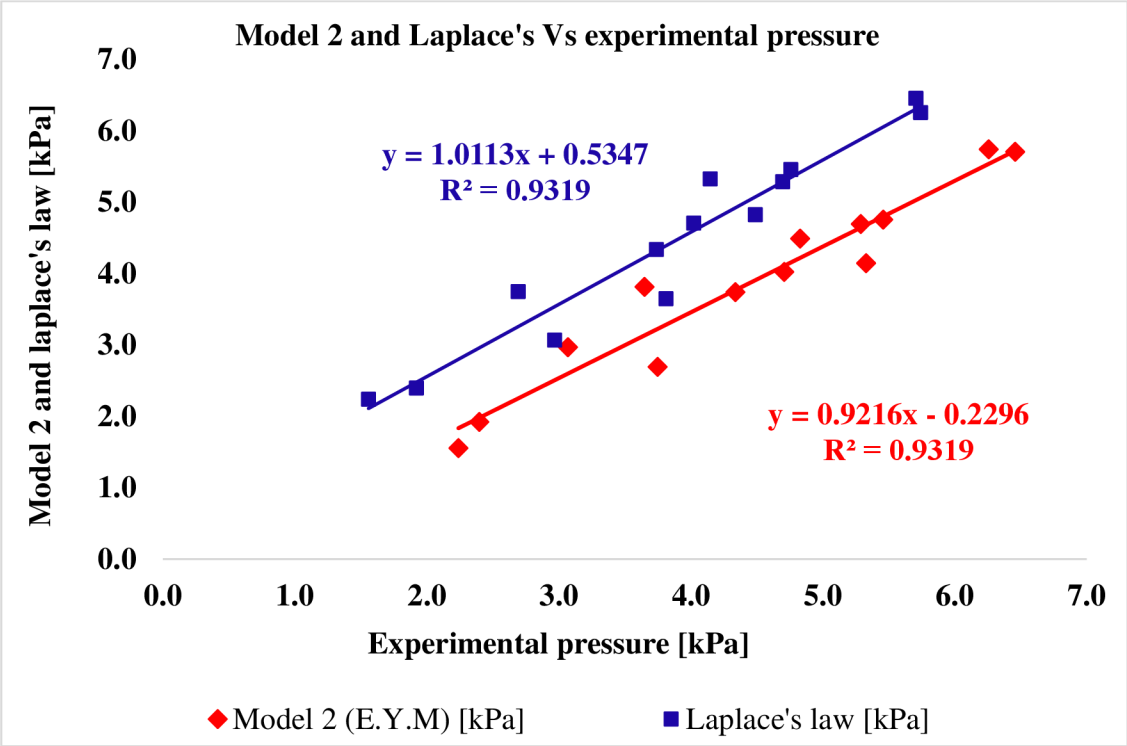

Figure 19. Experimental pressure compared to model 2 (E.Y.M) and Laplace's law

Table 7 portrays the statistical summary results of regression analysis between Model 1 (T.Y.M), Model 2 (E.Y.M), Laplace's law and experimental pressure based on coefficient of determination values showing that newly modified model's estimated results are very close to pressure predicted using Laplace's law

Table 7. Regression analysis summary of experimental pressure results compared to modified models and Laplace's law

Experimental pressure compared to modified models and Laplace's law	Regression model Y= bX + a b; slope and a; y-intercept	Coefficient of determination (R^2-value)
Model 1 (T.Y.M)	y = **0.9949 (experimental pressure) - 0.137**	R^2 = 0.9197
Model 2 (E.Y.M)	y = **1.0113 (experimental pressure) + 0.5347**	R^2 = **0.9319**
Laplace's law	y = **1.0113 (experimental pressure) + 0.5347**	R^2 = **0.9319**

7.7. Comparison of existing models and experimental pressure

Table 8 is illustrating the measured values of experimental pressure (Ps) to be compared with newly modified models; model 1 (T.Y.M) and model 2 (E.Y.M). Table 8 also comprised of pressure results calculated considering existing models developed in the past. Most of these models, based on the basic theory of Laplace's law, include; Hui's model (equation 9), Ng's model (equation 10), Meklewska's model (equation 12), Dubuis's model (equation 13), Leung's model (equation 14), Jariyapunya's model (equation 15), Zhang's model (equation 16), Teyeme's model (equation 17); and Laplace's law (equation 1) etc.

In this research, all existing models were compared to experimental pressure (Ps) results to estimate their strength of accuracy. The measured results of all models are given in table 8.

Table 8. Comparison of theoretical and experimental pressure values

Code	Experimental pressure [kPa]	Laplace's law [kPa]	Model 1 (T.Y.M) [kPa]	Model 2 (E.Y.M) [kPa]	Hui's model [kPa]	Ng's model [kPa]	Zhang's model [kPa]	Dubuis's model [kPa]	Leung's model [kPa]	Teyeme's model [kPa]	Jariyapunya's model [kPa]
A1	2.24	1.558	1.759	1.558	1.558	1.558	1.558	1.558	1.234	1.558	1.558
A2	2.4	1.922	2.079	1.922	1.922	1.922	1.922	1.788	1.385	1.922	1.922
A3	3.07	2.970	3.300	2.970	2.970	2.970	2.970	2.376	1.426	2.970	2.970
B1	3.65	3.815	4.291	3.815	3.815	3.815	3.815	4.120	2.678	3.815	3.815
B2	3.75	2.694	3.062	2.694	2.694	2.693	2.694	2.694	1.998	2.694	2.694
B3	4.34	3.741	4.208	3.741	3.741	3.741	3.741	4.040	2.761	3.741	3.741
C1	4.71	4.024	4.434	4.024	4.024	4.025	4.024	4.346	2.934	4.024	4.024
C2	4.83	4.491	5.132	4.491	4.491	4.491	4.491	4.311	2.802	4.491	4.491
C3	5.29	4.699	5.255	4.699	4.699	4.699	4.699	4.887	2.973	4.699	4.699
C4	5.33	4.149	4.610	4.149	4.149	4.148	4.149	4.149	3.077	4.149	4.149
C5	5.46	4.760	5.109	4.760	4.760	4.761	4.760	4.884	3.175	4.760	4.760
C6	6.26	5.742	6.380	5.742	5.742	5.742	5.742	5.742	3.493	5.742	5.742
C7	6.46	5.707	6.095	5.707	5.707	5.708	5.707	6.278	4.238	5.707	5.707

The relationship between existing models; Hui's model (equation 9), Ng's model (equation 10), Dubuis's model (equation 13), Leung's model (equation 14) and Zhang's model (equation 16), Teyeme's model (equation 17), and Jariyapunya's model (equation 15) as a predictors and experimental pressure as (response variable) was analyzed using linear regression analysis. Regression analysis of all existing models is discussed below simultaneously.

Hui's model; Figure 20 portrays the relationship between experimental pressure as predictor and Hui's model as a response variable. The strength of the relationship was quantified based on coefficient of determination value (R^2 -value = 0.9319). This value portrays that experimental pressure results explain 93.19% to Hui's model (equation 9). Table 9 depicts that Hui's model (equation 9) exerts lower pressure than experimental pressure but similar values to Laplace's law and modified models; model 1. These results portray that Hui's did not incorporate any new parameter instead of just notational changes defining the Laplace's law and conversion factor that is just for transformation from wooden leg to human leg. Regression model parameters; y-intercept is -0.2296 while slope is 0.9216 shows the line coinciding the point on y-axis and steepness of the regression line.

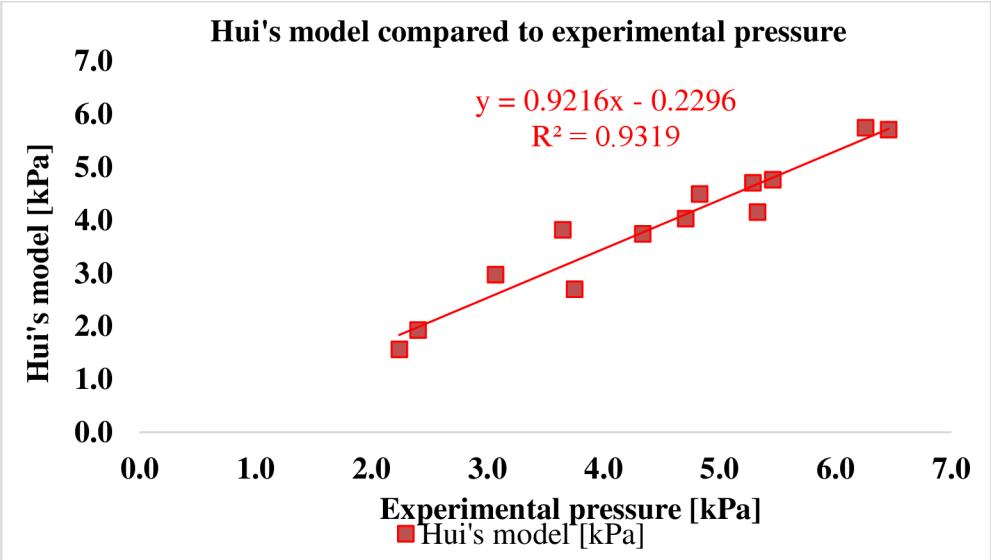

Figure 20. Comparison of experimental pressure compared to Hui's model

Ng's Model (equations 10) was analyzed for its efficacy to predict the compression pressure and extent of dependency on experimental pressure results using linear regression analysis (figure 21). Using linear regression analysis, the coefficient of determination value (R^2-value = 0.9318)

which means the experimental pressure results explain 93.18% to Ng's model. Table 9 portrays that Ng's model exerts the same pressure like Hui's model and Laplace's law except a very small difference in slope (0.9217) and y-intercept (0.2303) values. The additional parameters introduced by Ng was the reduction ratio (R_e) as a replacement of engineering strain.

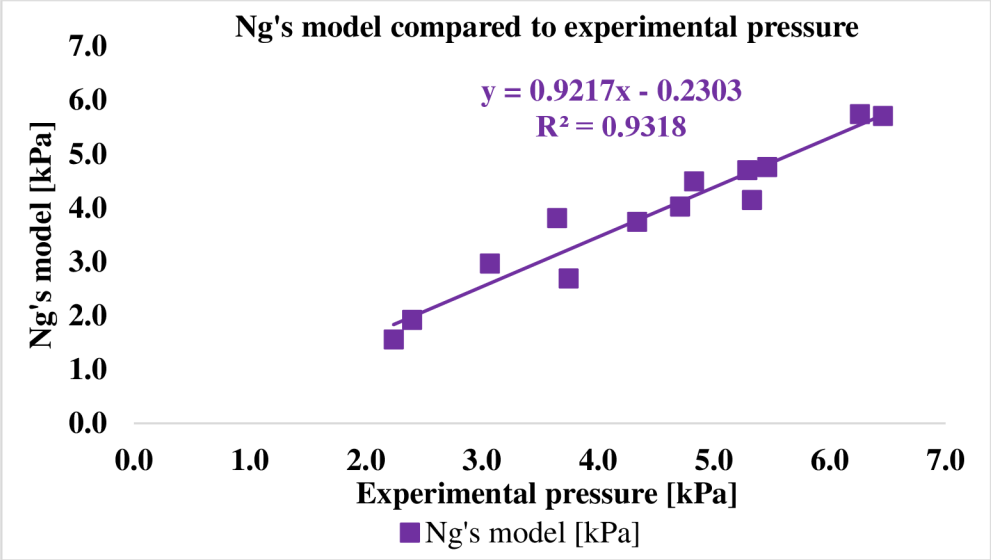

Figure 21. Comparison of experimental pressure compared to Ng's model

Dubuis's model was used for the investigation that how much the experimental results explain the Dubuis model based on the coefficient of determination (R^2-value= 0.9223) This shows that experimental pressure explains 92.23% to Dubuis's model (figure 22). Table 9 portrays that Dubuis's model pressure results are lower than experimental pressure. In his model (equation 13), it was introduced the concept of stiffness (Stiff) and engineering strain (ε) to predict the compression pressure incorporated to Laplace's law claiming the modification of Laplace's law but the extent the results of (R^2-value) was less than Hui's model, Ng's model and Laplace's law. The regression model parameters measured using least square method were y-intercept and slope exhibit the values -0.6153 and 1.0239 respectively.

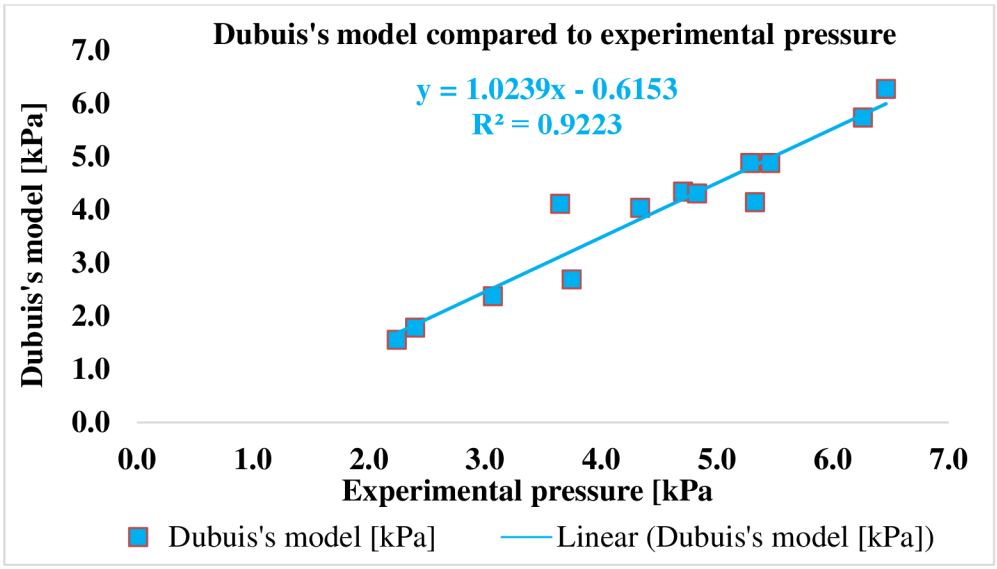

Figure 22. Comparison of experimental pressure compared to Dubuis's model

Leung's Model; Figure 23 shows the statistical relationship between experimental compression pressure results and Leung's model (equation 14). The extent of relationship was quantified by measuring the coefficient of determination value (R^2-value =0.9187).

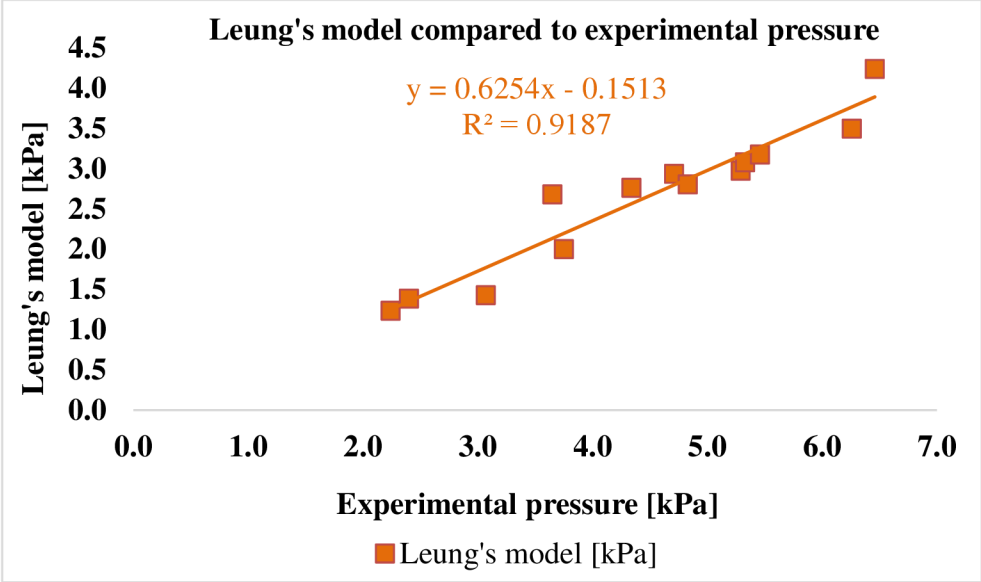

Figure 23. Comparison of experimental pressure compared to Leung's model

This value represents 91.87% significance between experimental pressure and Leung's model. Leung's model (equation 14) defined the tension (T) mentioned in Laplace's law (P=T/r) as T =

$F/\ell_o(1+\varepsilon)$ introduced the parameters additionally to predict the compression pressure. The coefficient of determination values measured using regression model is also lower than newly modified models; model 1 (R^2-value =0.9319) and model 2 (R^2-value =0.9319) as well as existing modes; Huis model (R^2-value =0.9319), Ng's model (R^2-value =0.9318), Dubuis's model (R^2-value =0.9223).

Zhang's Model; Figure 24 represents the strength of the relationship between experimental pressure (predictor) and Zhang's model (response variable).

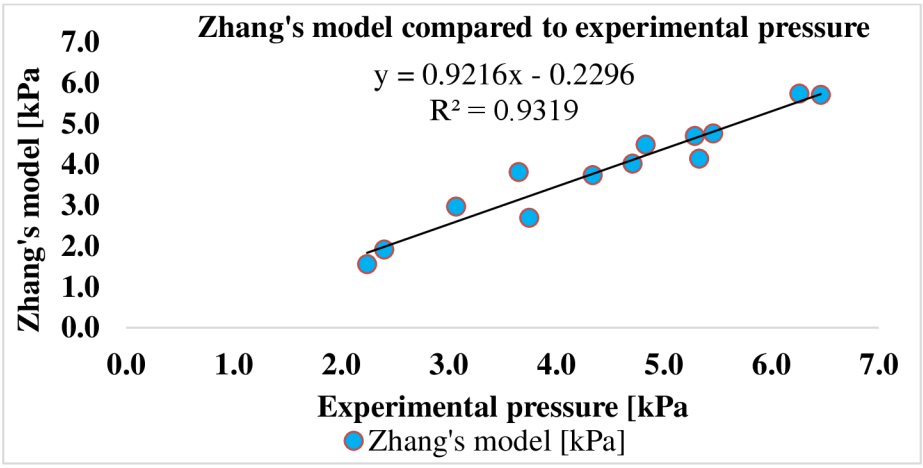

Figure 24. Comparison of experimental pressure compared to Zhang's model

The strength of the relationship was calculated based on coefficient of determination values (R^2 = 0.9319). This value portrays that experimental pressure explains 93.19% to Zhang's model. The regression parameters; y-intercept (-0.2296) and slope (0.9216) of Zhang's model exhibit similar value to Hui's model.

Teyeme's model was compared with experimental pressure based on coefficient of determination values (R^2-value= 0.9319) using linear regression analysis. This shows that experimental pressure explains 93.19% to Teyeme's model results (figure 25). Table 8 portrays that Teyeme's model results of pressure are lower than experimental pressure but similar to Laplace's law. In his model (equation 17), he considered that hooks law (F= - kX) is obeyed when socks are circumferentially stretched without considering the axial deformation.

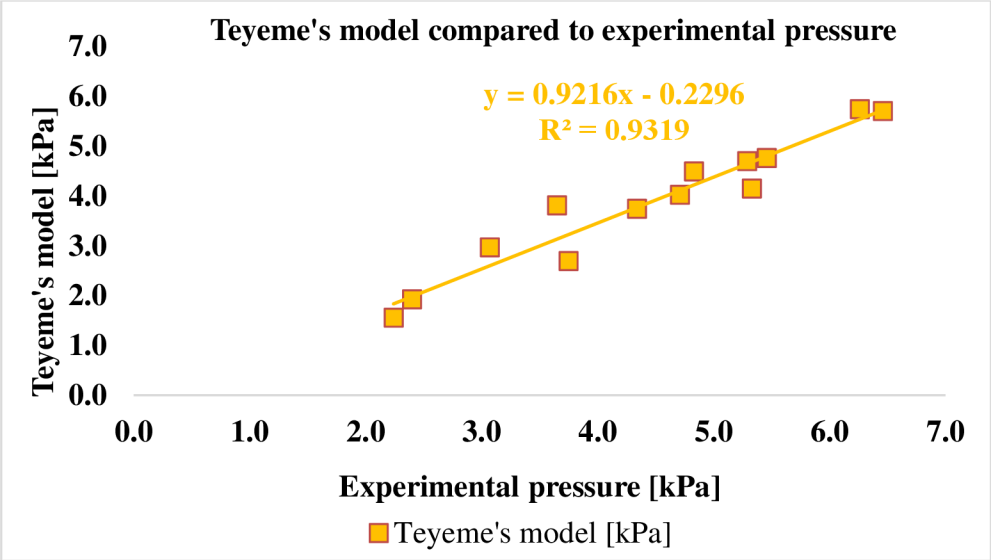

Figure 25. Comparison of experimental pressure compared to Teyeme's model

Jariyapunya's model; figures 26 represents the coefficient of determination value (R^2-value= 0.9319), y-intercept (-0.2296), and slope (0.9216) values determined by comparing the experimental pressure with Jariyapunya's model. R^2-value measured using Jariyapunya's model shows the results are similar to Laplace's law, Hui's model, Ng's model, Zhang's model, Teyeme's model and Dubuis's model.

Table 9 has portraying the summary of regression analysis based on the coefficient of the determination values of all of the existing models compared with experimental pressure results.

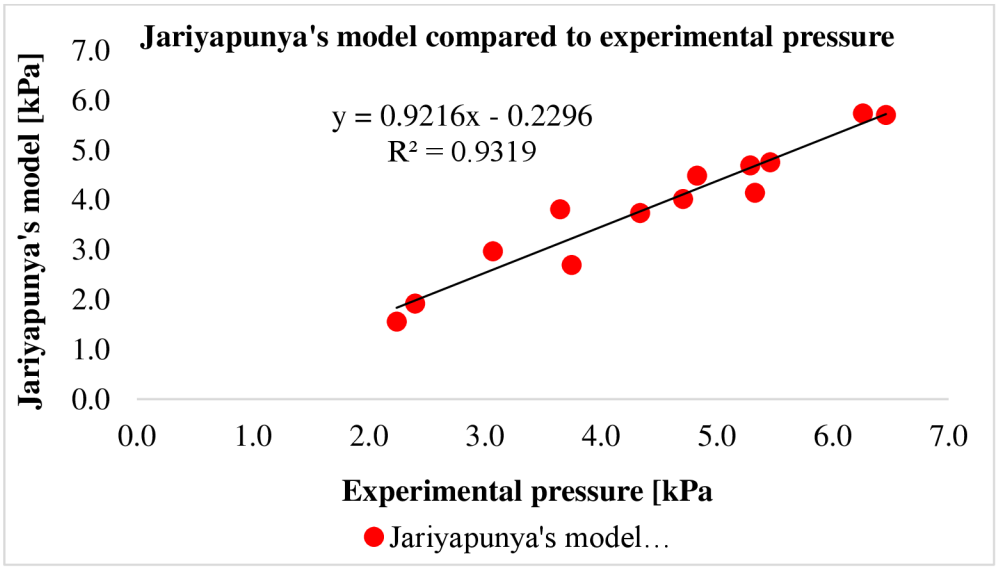

Figure 26. Comparison of experimental pressure compared to Jariyapunya's model

Table 9. Regression analysis summary of experimental pressure results compared to existing models

Experimental pressure compared to existing models	Regression model; Y= bX + a b; slope, a; y-intercept and X; experimental pressure	Coefficient of determination (R^2- value)
Hui's model	y = 0.9216(experimental pressure) - 0.2296	R^2 = 0.9319
Ng's model	y = 0.9217(experimental pressure) - 0.2303	R^2 = 0.9318
Dubuis's model	y = 1.0239(experimental pressure) - 0.6153	R^2 = 0.9223
Leung's model	y = 0.6254(experimental pressure) - 0.1513	R^2 = 0.9187
Zhang's model	y = 0.9216(experimental pressure) - 0.2296	R^2 = 0.9719
Teyeme's model	y = 0.9216(experimental pressure) - 0.2296	R^2 = 0.9719
Jariyapunya' s model	y = 0.9216(experimental pressure) - 0.2296	R^2 = 0.9319

7.8. Comparison of developed models and Laplace's law

In this scientific research, modified models; model 1 (T.Y.M) and model 2 (E.Y.M) were compared with the basic Laplace's law statistically to verify their mutual authenticity, significance or compatibility using simple linear regression analysis tool

Figure 27 portrays the relationship between Laplace's law as predictor and developed models; Model 1 (T.Y.M) and Model 2 (E.Y.M) as response variables. The strength of the relationship was measured based on the coefficient of the determination value (R^2-value). Coefficient of the determination value between Laplace's law and Model 1 (T.Y.M) was 0.9952 while between Laplace's law and Model 2 (E.Y.M) was equal to 1. These values; R^2= 0.9952 and R^2 =1 shows that Laplace's law explained Model 1 (T.Y.M) to 99.52 % while to Model 2 (E.Y.M) 100%. The results proved that modified models have well approximation to original Laplace's law. The regression model (figure 27) are comprised of two main parameters; y-intercept, a = 0.0932 (line coincides with y-axis) and the slope, b=1.0842 value (coefficient of predictor) of Model 1 (T.Y.M) and y-intercept, a = 0.0 (line coincides to origin) and the slope, b=1 value (coefficient of predictor) of Model 2 (E.Y.M). Here the slope represents the steepness of the line. Figure 27 proved the well approximation between Laplace's law and developed models; Model 1 (T.Y.M) and Model 2 (E.Y.M).

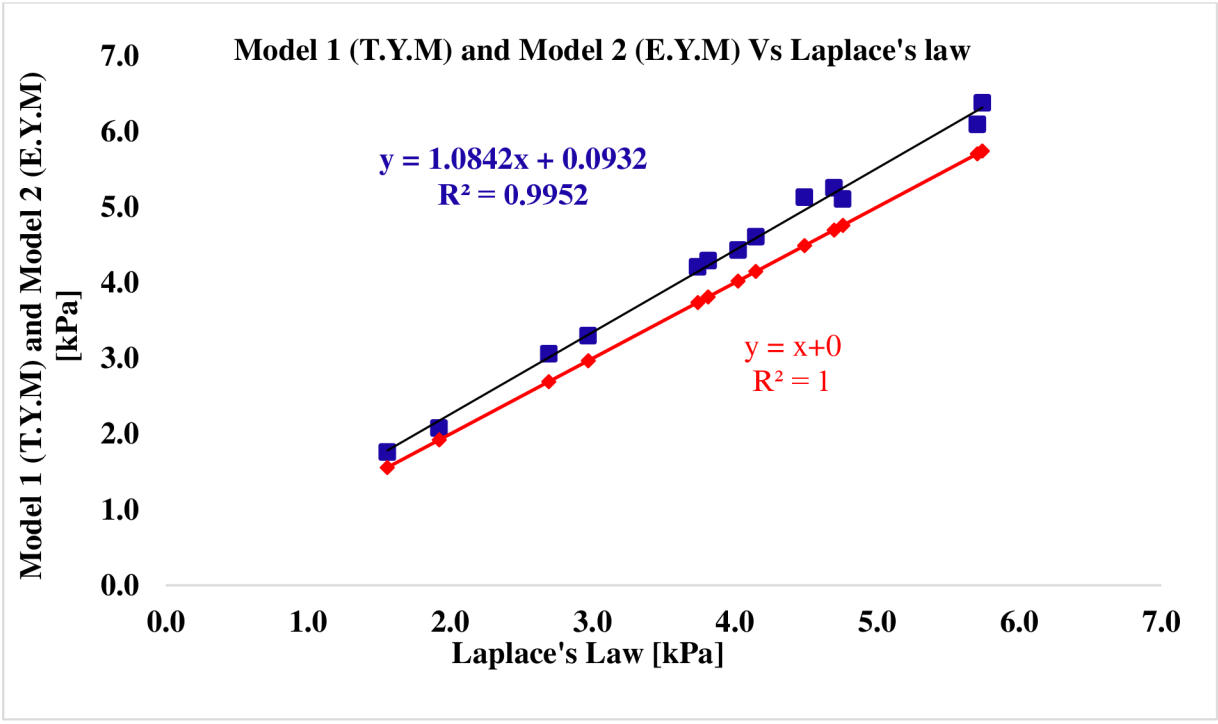

Figure 27. Comparison of developed models and Laplace's law

The summary results of the simple linear regression analysis between Laplace's law and newly developed models are given in table 10.

Table 10. Regression analysis summary between Laplace's law and modified models

Laplace's law compared to Newly developed models	**Regression model; Y= bX + a b; slope, a; y-intercept and X; Laplace's law pressure**	**Coefficient of determination (R^2- value)**
Model 1 (T.Y.M)	y = **1.0842** (Laplace's law pressure) **+ 0.0932**	R^2 = 0.9952
Model 2 (E.Y.M)	y = Laplace's law pressure	R^2 =1

8. Conclusions

In this scientific research work, it was concluded that;

Tensile properties of compression socks are of great importance to describe the engineering of compression socks. Many of these directly relate to present the intensity of exertion of compression pressure especially Hysteresis, loading energy, unloading energy, and tensile linearity.

Force at practical extension (F_L) values context to the circumferential difference between the socks and leg at the ankle portion have a strong relationship with the values of the experimental pressure (Ps). Tensile indices especially; hysteresis (H), loading energy (LE), unloading energy (UE), tensile linearity combined with the force at practical extension (F_L) portrayed a significant relationship to experimental pressure.

Two new mathematical models were developed by introducing the missing parameters ever introduced or incorporated for the prediction of compression pressure. These introduced parameters are true stress/true strain and true modulus along with the deformed width of ankle cut-strips considering the modelization technique.

Both of newly developed were statistically compared with the experimental pressure and existing models.

Developed models; model 1 (T.Y.M) and model 2 (E.Y.M) along with Laplace's law were compared with experimental pressure (Ps). Model 1 (T.Y.M) exhibits a slight less strength when compared to Laplace's law. While the model 2 (E.Y.M) exhibits the similar strength of the relationship with Laplace's law when was compared with experimental pressure.

Existing models were also compared to experimental pressure and found that Hui's model, Ng's model, Jariyapunya's model, Laplace's law, and Model 2 (E.Y.M) portrays the similar extent of the relationship exhibiting the different regression parameters (y-intercept and slope) values. From the existing models; Dubuis's model portrays the strength higher than model 1 (T.Y.M) and slightly lower than model 2 (E.Y.M). While Leung's model exhibits the strength lower than both modified models. Statistical analysis between existing models and developed models also portrays that Zhang's model and Teyeme's models exhibit the higher strength of the relationship than both modified models.

Developed models were also statistically compared with the Laplace's law to quantify their mutual strength of significant.

The strength of the relationship between modified models and basic Laplace's law was also quantified based on the coefficient of the determination values (R^2-value). Both of modified models; model 1 (T.Y.M) and model 2 (E.Y.M) have well explained the Laplace's law model exhibiting the highest value of the coefficient of the determination values; R2-value =0.9952 and R2-value =1 respectively. Conclusively, developed models predicts almost the same pressure results as Laplace's works.

9. Future work

In the future work tensile indices values (hysteresis, loading energy, unloading energy and tensile linearity) can be incorporated to predictor mathematical models based on the theory of Laplace's law.

As a future work, the cylindrical coordinate system should be used to develop mathematical models for the prediction of compression pressure

10. References

[1] FLAUD, Patrice, Sophie BASSEZ and Jean-Louis COUNORD. Comparative in vitro study of three interface pressure sensors used to evaluate medical compression hosiery. *Dermatologic Surgery* [online]. 2010, 36(12), 1930–1940 [accessed 2019-11-20]. ISSN 1524-4725. Available at: doi:10.1111/j.1524-4725.2010. 01767.x

[2] KHABURI, Jawad Al, Abbas A. DEHGHANI-SANIJ, E. Andrea NELSON and Jerry HUTCHINSON. Measurement of interface pressure applied by medical compression bandages. In: *2011 IEEE International Conference on Mechatronics and Automation* [online] 2011, s. 289–294 [accessed 2021-12-31].
Available at: doi:10.1109/ICMA.2011.5985672

[3] *Principles of compression in venous disease: A practitioner's guide to treatment and prevention of venous leg ulcers* [online]. B.m.: Wounds International, Enterprise House. květen 2013 [accessed 2021-12-15]. Available at: https://www.woundsinternational.com/resources/details/principles-compression-venous-disease-practitioners-guide-treatment-and-prevention-venous-leg-ulcers.

[4] *Consent: High Tie and Stripping Varicose Veins* [online]. B.m.: SurgeryMe Surgery. únor 2019 [accessed 2021-05-15]. Available at: https://teachmesurgery.com/consent/vascular/stripping-varicose-veins/.

[5] BS 6612:1985. *British Standard Specification for Graduated compression hosiery*. London: British Standards Institution. 1985.

[6] CERTIFICAT QUALITÉ-PRODUITS. *Référentiel technique prescrit pour les orthèses élastiques de contention des membres*. Paris: ASQUAL,. 1999.

[7] RAL DEUTSCHES INSTITUT FUR GUTESICHERUNG UND KENNZEICHNUNG E.V. *Medical compression hosiery—Quality assurance RAL-GZ 387/1*. B.m.: RAL Deutsches Institut fur Gutesicherung und Kennzeichnung e.V. 2008.

[8] CLARK, Michael and G. KRIMMEL. Lymphoedema and the construction and classification of compression hosiery. *Lymphoedema Framework. Template for Practice: Compression hosiery in lymphoedema* [online]. 2006, 2–4. Available at: https://www.lympho.org/wp-content/uploads/2021/09/Compression_hosiery.pdf

[9] BERA, Mukesh Kumar, Rabisankar CHATTOPADHAY and Deepti GUPTA. The effect of fibre blend on comfort characteristics of elastic knitted fabrics used for pressure garments. *Journal of The Institution of Engineers (India): Series E* [online]. 2014, 95(1), 41–47 [accessed 2020-06-29]. ISSN 2250-2491. Available at: doi:10.1007/s40034-014-0029-x

[10] SAU-FUN, Ng, Hui CHI-LEUNG and Wong LAI-FAN. Development of medical garments and apparel for the elderly and the disabled. *Textile Progress* [online]. 2011, 43(4), 235–285 [accessed 2021-06-02]. ISSN 0040-5167. Available at: doi:10.1080/00405167. 2011.-573240

[11] MACINTYRE, Lisa, Margot BAIRD and Phil WEEDALL. The study of pressure delivery for hypertrophic scar treatment. *International Journal of Clothing Science and Technology* [online]. 2004, 16(1/2), 173–183 [accessed 2022-03-29]. ISSN 0955-6222. Available at: doi:10.1108/09556220410520450

[12] SAU-FUN, Ng, Hui CHI-LEUNG. Model to Predict Interfacial Pressures in Multilayer Elastic Fabric Tubes. *Textile Research Journal* [online]. 2001, 71(8), 683–687 [accessed 2022-08-18]. ISSN 1746-7748. Available at: doi:10.1177/004051750107100806

[13] SCHUREN, Jan. and Kay. MOHR. Pascal's law and the dynamics of compression therapy: a study on healthy volunteers. *International Angiology* [online]. 2010, 29(5), 431–435 [accessed 2022-04-26]. ISSN 1827-1839.
Available at: https://pubmed.ncbi.nlm.nih.gov/20924347/

[14] DAI, X.Q., Yi LI, Rong LIU and Yi Lin KWOK. Biomechanical engineering of compression stockings. In: *Biomechanical Engineering of Textiles and Clothing*. B.m.: Elsevier Inc, 2006, s. 332–346. ISBN 978-1-84569-148-6.

[15] TSUJISAKA, Toshiyuki, Yoshiaki AZUMA, Yo-Ichi MATSUMOTO and Hideo MOROOKA. Comfort pressure of the top part of men's socks. *Textile Research Journal* [online]. 2004, 74(7), 598–602 [accessed 2019-12-20]. ISSN 1746-7748. Available at: doi:10.1177/004051750407400707

[16] NAVE, Carl Rod. *Wall Tension* [online]. 1998 [accessed 2021-05-15]. Available at: http://hyperphysics.phy-astr.gsu.edu/hbase/ptens.html.

[17] HOPKINS, Alison and Fran WORBOYS. Understanding compression therapy to achieve tolerance. *Wounds UK* [online]. 2005, 1(3), 26–34. ISSN 1746-6814. Available at: https://www.wounds-uk.com/journals/issue/4/articledetails/understandingcompression-therapy-to-achieve-tolerance-1

[18] VAN DER WEGEN-FRANKEN, Karin, Wim ROEST, Bhupendra TANK and Martino NEUMANN. Calculating the pressure and the stiffness in three different categories of class ii medical elastic compression stockings. *Dermatologic Surgery* [online]. 2006, 32(2), 216–223 [accessed 2021-07-24]. ISSN 1524-4725. Available at: doi:10.1111/j.1524-4725.2006. 32040.x

[19] LIU, Rong, Terence T.H. LAO and Xin WANG. Impact of weft laid-in structural knitting design on fabric tension behavior and interfacial pressure performance of circular knits. *Journal of Engineered Fibers and Fabrics* [online]. 2013, 8(4), 96–107 [accessed 2020-05-15]. ISSN 1558-9250. Available at: doi:10.1177/155892501300800404

[20] LIU, Rong., Yi-Lin. KWOK, Yi LI, Terence-T.H. LAO and Xin ZHANG. Quantitative Assessment of Relationship between Pressure Performances and Material Mechanical Properties of Medical Graduated Compression Stockings. *Journal of Applied Polymer Science* [online]. 2007, 104(1), 601–610 [accessed 2020-07-07]. ISSN 1097-4628. Available at: doi:10.1002/app.25617

[21] LIU, Rong. *Comfort and mechanical function of compression stockings*. B.m., 2006. PhD Thesis. Hong Kong Polytechnic University.

[22] LIU, Rong, Yi-Lin KWOK, Yi LI, Terence-T.H. LAO, Xin ZHANG and Xiao Qun DAI. Objective evaluation of skin pressure distribution of graduated elastic compression stockings. *Dermatologic Surgery* [online]. 2005, 31(6), 615–624. ISSN 1076-0512. Available at: doi:10.1097/00042728-200506000-00001

[23] LIU, Rong, Yi-Lin KWOK, Yi LI and Terence T.H LAO. Fabric mechanical-surface properties of compression hosiery and their effects on skin pressure magnitudes when worn. *Fibres and Textiles in Eastern Europe*. 2010, 79(2), 91–97. ISSN 1230-3666.

[24] LIU, Rong, Yi-Lin KWOK, Yi LI, Terence-T.H. LAO, Xin ZHANG and Xiao Qun DAI. A three-dimensional biomechanical model for numerical simulation of dynamic pressure functional performances of graduated compression stocking (GCS). *Fibers and Polymers* [online]. 2006, 7(4), 389–397 [accessed 2021-02-20]. ISSN 1875-0052. Available at: doi:10.1007/BF02875771

[25] ZHANG, Mei, Henan DONG, Xuerong FAN and Rui DAN. Finite element simulation on clothing pressure and body deformation of the top part of men's socks using curve fitting equations. *International Journal of Clothing Science and Technology* [online]. 2015, 27(2), 207–220 [accessed 2021-04-04]. ISSN 0955-6222. Available at: doi:10.1108/IJCST-12-2013-0139

[26] KERMAVNAR, Tjaša, Valerie POWER, Adam DE EYTO and Leonard W. O'SULLIVAN. Computerized cuff pressure algometry as guidance for circumferential tissue compression for wearable soft robotic applications: A systematic review. *Soft Robotics* [online]. 2018, 5(1), 1–16 [accessed 2022-01-28]. ISSN 2169-5172. Available at: doi:10.1089/soro.2017.0046

[27] BRUNIAUX, Pascal, David CREPIN and Bertrand LUN. Modeling the mechanics of a medical compression stocking through its components behavior: Part 1 – modeling at the yarn scale. *Textile Research Journal* [online]. 2012, 82(18), 1833–1845 [accessed 2020-06-27]. ISSN 1746-7748. Available at: doi:10.1177/0040517512441992

[28] ZHANG, Xinyue, K.W. YEUNG and Yi LI. Numerical simulation of 3d dynamic garment pressure. *Textile Research Journal* [online]. 2002, 72(3), 245–252 [accessed 2020-10-03]. ISSN 1746-7748. Available at: doi:10.1177/004051750207200311

[29] YANMEI, Li, Zhang WEIWEI, Ju FAN and Han QINGYUN. Study on clothing pressure distribution of calf based on finite element method. *The Journal of The Textile Institute* [online]. 2014, 105(9), 955–961 [accessed 2021-10-30]. ISSN 0040-5000. Available at: doi:10.1080/00405000.2013.865883

[30] SOLTANZADEH, Zeynab, Saeed SHAIKHZADEH NAJAR, Mohammad HAGHPANAHI and Mohammd Reza MOHAJERI-TEHRANI. Prediction of compression properties of single jersey weft-knitted fabric by finite element analysis based on the hyperfoam material model. *Fibres and Textiles in Eastern Europe* [online]. nedatováno, 24(2 (116)), 82–88 [accessed 2021-03-29]. ISSN 1230-3666. Available at: doi: 10.5604/ 1 2-303666.1191431

[31] FRAUZIOLS, Fanny, Jérôme MOLIMARD, Laurent NAVARRO, Pierre BADEL, Magalie VIALLON, Rodolphe TESTA and Stéphane AVRIL. Prediction of the biomechanical effects of compression therapy by finite element modeling and ultrasound elastography. *IEEE Transactions on Biomedical Engineering* [online]. 2015, 62(4), 1011–1019 [accessed 2022-06-20]. ISSN 1558-2531. Available at: doi:10.1109/TBME. 20 1 4 . 2378553

[32] YU, Annie, Kit Lun YICK, Sun Pui NG, Joanne YIP and Ying Fan CHAN. Numerical simulation of pressure therapy glove by using Finite Element Method. *Burns : journal of the International Society for Burn Injuries* [online]. 2016, 42(1), 141–151 [accessed 2021-09-19]. ISSN 0305-4179. Available at: doi:10.1016/j.burns.2015.09.013

[33] DAN, Rui, Xue-rong FAN, Zhen SHI and Mei ZHANG. Finite element simulation of pressure, displacement, and area shrinkage mass of lower leg with time for the top part of men's socks. *The Journal of The Textile Institute* [online]. 2015, 107(1), 72–80 [accessed 2022-05-22]. ISSN 0040-5000.Available at: doi:10.1080/00405000.2015.100 7 6-21

[34] CHASSAGNE, Fanette, Jerome MOLIMARD, Reynald CONVERT, Pascal GIRAUX and Pierre BADEL. Numerical model reduction for the prediction of interface pressure applied by compression bandages on the lower leg. *IEEE transactions on bio-medical engineering* [online]. 2018, 65(2), 449–457 [accessed 2019-05-09]. ISSN 1558-2531. Available at: doi: 10.1109/TBME.2017.2774598

[35] European committee for standardization (CEN) non-active medical devices. *ENV 12718:2001 - Medical compression hosiery*. B.m.: Brussels, CEN/TC205. srpen 2001.

[36] LIU, Rong, Terence T.H. LAO, Trevor J LITTLE, Xinbo WU and Xiao KE. Can heterogeneous compression textile design reshape skin pressures? A fundamental study. *Textile Research Journal* [online]. 2018, 88(17), 1915–1930 [accessed 2020-11-22]. ISSN 1746-7748. Available at: doi:10.1177/0040517518779254

[37] SARI, Burak and Nida OĞLAKCIOĞLU. Analysis of the parameters affecting pressure characteristics of medical stockings. *Journal of Industrial Textiles* [online]. 2018, 47(6), 1083–16 [accessed 2020-06-09]. ISSN 1528-0837. Available at: doi:10.1177/15280837-16662587

[38] MAKLEWSKA, Elżbieta, Andrzej NAWROCKI, Jolanta LEDWOŃ and Krzysztof KOWALSKI. Modelling and designing of knitted products used in compressive therapy. *Fibres and Textiles in Eastern Europe* [online]. 2006, 14(5 (59)), 111–113. ISSN 2300-7354. Available at: http://www.fibtex.lodz.pl/article1128.html

[39] CHOI, Ka-Fai, Ameersing LUXIMON. Contact pressure of tubular fabrics for compression sportswear. In: *Proceedings of Textile Bioengineering and Informatics Symposium Vol.1-3*. 2010, s. 1425–1429.

[40] JARIYAPUNYA, Nareerut and Blažena MUSILOVÁ. Predictive modelling of compression garments for elastic fabric and the effects of pressure sensor thickness. *The Journal of The Textile Institute* [online]. 2019, 110(8), 1132–1140 [accessed 2022-07-15]. ISSN 0040-5000. Available at: doi:10.1080/00405000.2018.1540285

[41] TEYEME, Yetanawork, Benny MALENGIER, Tamrat TESFAYE, Simona VASILE, Wolelaw ENDALEW and Lieva VAN LANGENHOVE. Predicting compression pressure of knitted fabric using a modified laplace's law. *Materials* [online]. 2021, 14(16), 4461 [accessed 2022-03-25]. ISSN 1996-1944. Available at: doi:10.3390/ma14164461

[42] ZHANG, Luolan, Guangwu SUN, Jiecong LI, Yu CHEN, Xiaona CHEN, Weihong GAO and Wenfeng HU. The structure and pressure characteristics of graduated compression stockings: experimental and numerical study. *Textile Research Journal* [online]. 2019, 89(23–24), 5218–5225 [accessed 2021-11-21]. ISSN 1746-7748. Available at: doi:10. 117 -7/0040517519855319

[43] COSTANZO, Francesco and James G. BRASSEUR. The invalidity of the Laplace law for biological vessels and of estimating elastic modulus from total stress vs. strain: a new practical method. *Mathematical Medicine and Biology: A Journal of the IMA* [online]. 2015, 32(1), 1–37 [accessed 2021-11-22]. ISSN 1477-8599.Available at: doi:10.1093/ i m ammb/-/dqt020

[44] NG, Sau-Fun. and Chi-Leung HUI. Pressure model of elastic fabric for producing pressure garments. *Textile Research Journal* [online]. 2001, 71(3), 275–279 [accessed 2021-05-03]. ISSN 1746-7748. Available at: doi:10.1177/004051750107100314

[45] LIU, Rong, Yi-Lin KWOK, Yi LI, Terence T. LAO and Xin ZHANG. Skin pressure profiles and variations with body postural changes beneath medical elastic compression stockings. *International Journal of Dermatology* [online]. 2007, 46(5), 514–523

[accessed 2020-02-19]. ISSN 1365-4632. Available at: doi:10.1111/j.1365-4632. 2007.0 3 175.x

[46] CIEŚLAK, Małgorzata, Agnieszka KARASZEWSKA, Ewa GROMADZIŃSKA, Izabela JASIŃSKA and Irena KAMIŃSKA. Comparison of methods for measurement of the pressure exerted by knitted fabrics. *Textile Research Journal* [online]. 2017, 87(17), 2117–2126 [accessed 2021-07-29]. ISSN 1746-7748.Available at: doi:10.1177/0040517516665-255

[47] HALFAOUI, Rachid. and Bachir. CHEMANI. New approach to predict pressure produced by elastic textile in the therepeutic treatment of venous leg. *Journal of Fundamental and Applied Sciences* [online]. 2016, 8(2), 297–312 [accessed 2020-01-27]. ISSN 1112-9867. Available at: doi:10.4314/jfas.v8i2.9

[48] LEUNG, W. Y., D. W. YUEN, Sun Pui NG and S. Q. SHI. Pressure prediction model for compression garment design. *Journal of Burn Care & Research* [online]. 2010, 31(5), 716–727 [accessed 2021-11-29]. ISSN 1559-047X. Available at: doi:10.1097/BCR.0b01 3e318-1eebea0

[49] DUBUIS, Laura, Pierre-yves ROHAN, Stéphane AVRIL, Pierre BADEL and Johan DEBAYLE. Patient-specific FE model of the leg under elastic compression. In: *10th International Symposium on Computer Methods in Biomechanics and Biomedical Engineering*. 2012, s. 1–7.

[50] XIONG, Ying and Xiaoming TAO. Compression garments for medical therapy and sports. *Polymers* [online]. 2018, 10(6), 663 [accessed 2019-11-14]. ISSN 2073-4360. Available at: doi:10.3390/polym10060663

[51] VAN DER WEGEN-FRANKEN, C.P.M., Bhupendra TANK, Tamar NIJSTEN and H.A.M. NEUMANN. Changes in the pressure and the dynamic stiffness index of medical elastic compression stockings after having been worn for eight hours: a pilot study. *Phlebology* [online]. 2009, 24(1), 31–37 [accessed 2020-01-24]. ISSN 0268-3555. Available at: doi:10.1258/phleb.2008.008037

[52] VAN DER WEGEN-FRANKEN, Karin, Bhupendra TANK and Martino NEUMANN. Correlation between the static and dynamic stiffness indices of medical elastic compression stockings. *Dermatologic Surgery* [online]. 2008, 34(11), 1477–1485 [accessed 2021-07-09]. ISSN 1524-4725. Available at: doi:10.1111/j.1524-4725.2008.34312.x

[53] LIU, Rong, Xia GUO, Terence T.H., LAO and Trevor LITTLE. A critical review on compression textiles for compression therapy: Textile-based compression interventions for chronic venous insufficiency. *Textile Research Journal* [online]. 2017, 87(9), 1121–1141 [accessed 2021-11-11]. ISSN 1746-7748. Available at: doi:10.1177/0040517516646041

[54] NEUMANN, H. A. Martino. Elasticity, hysteresis and stiffness: the magic triangle. *Veins and Lymphatics* [online]. 2013, 2(1), 17–18 [accessed 2020-12-19]. ISSN 2279-7483. Available at: doi:10.4081/vl.2013.e6

[55] LIU, Rong, Yi-Lin KWOK, Yi LI, Terence-T LAO and Xin ZHANG. Effects of material properties and fabric structure characteristics of graduated compression stockings (GCS) on the skin pressure distributions. *Fibers and Polymers* [online]. 2005, 6(4), 322–331 [accessed 2021-01-31]. ISSN 1875-0052. Available at: doi:10.1007/BF02875669

[56] LIM, Chung Sim and Alun H. DAVIES. Graduated compression stockings. *Canadian Medical Association Journal* [online]. 2014, 186(10), E391 [accessed 2020-02-15]. ISSN 0820-3946. Available at: doi:10.1503/cmaj.131281

[57] PARTSCH, Hugo. Mechanism and effects of compression therapy. In: John J. BERGAN, ed. *The Vein Book* [online]. Burlington: Academic Press, 2007, s. 103–109. ISBN 978-0-12-369515-4. Available at: doi:10.1016/B978-012369515-4/50013-2

[58] HARPA, Rodica, Cristina PIROI and Cezar DORU RADU. A new approach for testing medical stockings. *Textile Research Journal* [online]. 2010, 80(8), 683–695 [accessed 2020-01-04]. ISSN 1746-7748. Available at: doi:10.1177/0040517509343781

[59] WANG, Yongrong, Peihua ZHANG and Yiping ZHANG. Experimental investigation the dynamic pressure attenuation of elastic fabric for compression garment. *Textile Research*

Journal [online]. 2014, 84(6), 572–582 [accessed 2020-04-23]. ISSN 1746-7748. Available at: doi:10.1177/0040517513503726

[60] LYLE, Dorothy Siegert. *Performance of Textiles*. New York: Wiley, 1977. ISBN 978-0-471-01418-8.

[61] HUI, Chi-Leung and Sau-Fun NG. Theoretical analysis of tension and pressure decay of a tubular elastic fabric. *Textile Research Journal* [online]. 2003, 73(3), 268–272. ISSN 1746-7748. Available at: doi:10.1177/004051750307300312

[62] WANG, Lijing, Martin FELDER and Jackie Y. CAI. Study of properties of medical compression fabrics. *Journal of Fiber Bioengineering and Informatics* [online]. 2011, 4(1), 15–22 [accessed 2021-03-19]. ISSN 1940-8676. Available at: doi:10.3993/jfbi04201102

[63] PARTSCH, Hugo. The use of pressure changes on standing as a surrogate measure of the stiffness of a compression bandage. *European Journal of Vascular and Endovascular Surgery* [online]. 2005, 30(4), 415–421 [accessed 2020-05-27]. ISSN 1078-5884. Available at: doi:10.1016/j.ejvs.2005.06.002

[64] STOLK, R., C. P. M. WEGEN VAN DER-FRANKEN and H. A. M. NEUMANN. A method for measuring the dynamic behavior of medical compression hosiery during walking. *Dermatologic Surgery* [online]. 2004, 30(5), 729–736 [accessed 2022-01-21]. ISSN 1524-4725. Available at: doi:10.1111/j.1524-4725.2004.30203.x

[65] HIRAI, Masafumi, K NIIMI, K MIYAZAKI, H IWATA, I SUGIMOTO, H ISHIBASHI, T OTA a Y KOMINAMI. Development of a device to determine the stiffness of elastic garments and bandages. *Phlebology* [online]. 2011, 26(7), 285–291 [accessed 2019-10-14]. ISSN 0268-3555. Available at: doi:10.1258/phleb.2010.010041

[66] PARTSCH, Hugo, Michael CLARK, Sophie BASSEZ, Jean-Patrick BENIGNI, Francois BECKER, Vladimír BLAŽEK, Joseph CAPRINI, André CORNU-THÉNARD, Jürg HAFNER, Mieke FLOUR, Michael JÜNGER, Christine MOFFATT and Martino NEUMANN. Measurement of lower leg compression in vivo: recommendations for the performance of measurements of interface pressure and stiffness. *Dermatologic Surgery*

[online]. 2006, 32(2), 224–233 [accessed 2020-02-26]. ISSN 1524-4725. Available at: doi:10.1111/j.1524-4725.2006.32039.x

[67] CORNU-THENARD, André, Jean-Patrick BENIGNI and Jean-François UHL. Terminology: resistance or stiffness for medical compression stockings? *Veins and Lymphatics* [online]. 2013, 2(1), 11–12 [accessed 2020-08-17]. ISSN 2279-7483. Available at: doi:10.4081/vl.2013.e4

[68] PARTSCH, Hugo, Michael CLARK, Giovanni MOSTI, Erik STEINLECHNER, Jan SCHUREN, Martin ABEL, Jean-Patrick BENIGNI, Philip COLERIDGE-SMITH, Andre CORNU-THÉNARD, Mieke FLOUR, Jerry HUTCHINSON, John GAMBLE, Karin ISSBERNER, Michael JUENGER, Christine MOFFATT, H. a. M. NEUMANN, Eberhard RABE, Jean F. UHL and Steven ZIMMET. Classification of compression bandages: practical aspects. *Dermatologic Surgery* [online]. 2008, 34(5), 600–609 [accessed 2021-05-05]. ISSN 1524-4725. Available at: doi:10.1111/j.1524-4725.2007.34116.x

[69] LURIE, Fedor and Robert L. KISTNER. Variability of interface pressure produced by ready-to-wear compression stockings. *Phlebology* [online]. 2014, 29(2), 105–108 [accessed 2019-09-12]. ISSN 0268-3555. Available at: doi:10.1258/phleb.2012.012045

[70] ANCUTIENE, Kristina, Marie KOLDINSKÁ and Antonín HAVELKA. Investigation of tensile resilience properties of stretch denim fabrics. *Indian Journal of Fibre & Textile Research* [online]. 2017, 42(2), 175–182 [accessed 2021-02-02]. ISSN 0975-1025. Available at: doi:10.56042/ijftr.v42i2.9857

[71] VARGHESE, Nirmala and G. THILAGAVATHI. Handle and comfort characteristics of cotton core spun polyurethane and polyester/polyurethane fabrics for application as blouse. *Journal of Textile and Apparel, Technology and Management* [online]. 2014, 8(4), 1–13 [accessed 2020-06-03]. ISSN 1533-0915. Available at:https://ojs.cnr.ncsu.edu/index.php/-JTATM/article/view/5341

[72] KAWABATA, Sueo. *The standardization and analysis of hand evaluation*. 2nd. ed. Osaka, Japan: Hand evaluation and standardization committee, Textile Machinery Society of Japan, 1980.

[73] BARTKOWIAK, Grażyna, Iwona FRYDRYCH, Agnieszka KOMISARCZYK and Agnieszka GRESZTA. Fabric selection for the reference clothing destined for ergonomics test of protective clothing— Sensorial comfort point of view. *Autex Research Journal* [online]. 2017, 17(4), 303–312 [accessed 2020-08-24]. ISSN 2300-0929. Available at: doi:10.1515/aut-2016-0033

[74] YAMADA, Tomoko and Masaru MATSUO. Clothing pressure of knitted fabrics estimated in relation to tensile load under extension and recovery processes by simultaneous measurements. *Textile Research Journal* [online]. 2009, 79(11), 1021–1033 [accessed 2020-12-23]. ISSN 1746-7748. Available at: doi:10.1177/0040517508099387

[75] ITO, Noriko, Mari INOUE, Masae NAKANISHI and Masako NIWA. The relation among the biaxial extension properties of girdle cloths and wearing comfort and clothing pressure of girdles. *Journal of the Japan Research Association for Textile End-Uses* [online]. 1995, 36(1), 102–108 [accessed 2019-04-12]. ISSN 0037-2072. Available at: doi:10.11419/sens-hoshi1960.36.102

[76] WANG, Yongrong, Yinhua CUI, Peihua ZHANG, Xunwei FENG, Jianming SHEN and Qiuyuan XIONG. A smart mannequin system for the pressure performance evaluation of compression garments. *Textile Research Journal* [online]. 2011, 81(11), 1113–1123 [accessed 2021-03-05]. ISSN 1746-7748. Available at: doi:10.1177/0040517511398942

[77] LIU, Rong, Terence T. LAO and Shu-xiao WANG. Technical knitting and ergonomical design of 3D seamless compression hosiery and pressure performances in vivo and in vitro. *Fibers and Polymers* [online]. 2013, 14(8), 1391–1399 [accessed 2021-06-23]. ISSN 1875-0052. Available at: doi:10.1007/s12221-013-1391-x

[78] TROYNIKOV, Olga, Elnaz ASHAYERI, Michael BURTON, Aleksandar SUBIC, Firoz ALAM and S. MARTEAU. Factors influencing the effectiveness of compression garments used in sports. *Procedia Engineering* [online]. 2010, 2(2), The Engineering of Sport 8 - Engineering Emotion, 2823–2829 [accessed 2019-11-15]. ISSN 1877-7058.Available at: doi:10.1016/j.proeng.2010.04.073

[80] CHEN, Dongsheng, Hong, LIU, Qiaoling ZHANG and Hongge WANG. Effects of mechanical properties of fabrics on clothing pressure. *Przegląd Elektrotechniczny*. 2013, 89(01b/2013), 232–235. ISSN 0033-2097.

[81] CHATTOPADHYAY, Rabisankar, Deepti GUPTA and Mukesh Kumar. BERA. Effect of input tension of inlay yarn on the characteristics of knitted circular stretch fabrics and pressure generation. *The Journal of The Textile Institute* [online]. 2012, 103(6), 636–642 [accessed 2021-11-12]. ISSN 0040-5000. Available at: doi:10.1080/00405000.2012.665-23

[82] TAMOUE, Ferdinand and Andrea EHRMANN. First principle study: parametric investigation of the mechanics of elastic and inelastic textile materials for the determination of compression therapy efficacy. *Textile Research Journal* [online]. 2018, 88(21), 2506-2515 [accessed 2019-05-10]. ISSN 1746-7748. Available at: doi:10.1177/-004051717725123

[83] HEGARTY, Meghan Sarah. *Technology for Continuously Monitoring the Effectiveness of Compression Therapy for Improving Patient Outcome*. B.m., 2013. PhD Thesis. North Carolina State University.

[84] HEGARTY-CRAVER, Meghan, Cassandra KWON, William OXENHAM, Edward GRANT and Lawrence REID. Towards characterizing the pressure profiles of medical compression hosiery: an investigation of current measurement devices and techniques. *The Journal of The Textile Institute* [online]. 2015, 106(7), 757–767 [accessed 2020-08-21]. ISSN 0040-5000. Available at: doi:10.1080/00405000.2014.941535

[85] ROYLANCE, Daaccessed *Stress-Strain Curves* [online]. B.m.: Massachusetts Institute of Technology. srpen 2001 [accessed 2019-09-22]. Available at: https://resources.saylor.org /wwwresources/archived/site/wp-content/uploads/2012/09/ME1022.2.4.pdf.

[86] KWON, Cassandra Hyun. *Characterizing the Relationship of Tensile Properties and Pressure Profiles of Compression Bandages and Fabrics*. B.m., 2014. PhD Thesis. North Carolina State University.

[87] LAKES, R. S. and A. WINEMAN. On poisson's ratio in linearly viscoelastic solids. *Journal of Elasticity* [online]. 2006, 85(1), 45–63 [accessed 2019-11-30]. ISSN 1573-2681. Available at: doi:10.1007/s10659-006-9070-4

[88] LIN, Yinglei, Kai-Fi CHOI, Ameersing LUXIMON, Lei YAO, JY HU and Y. LI. Finite element modeling of male leg and sportswear: contact pressure and clothing deformation. *Textile Research Journal* [online]. 2011, 81(14), 1470–1476 [accessed 2019-08-12]. ISSN 1746-7748. Available at: doi:10.1177/0040517510395997

[89] HIGUCHI, Kenji and Hideo TAKAI. Stress-strain diagram, young's modulus and poisson's ratio of textile fibers. *Journal of the Textile Machinery Society of Japan* [online]. 1961, 7(1), 4–12 [accessed 2022-12-01]. ISSN 0040-5043. Available at: doi:10.4188/jte-1955.7.4

[90] MILITKÝ, Jiří, Mohanapriya VENKATARAMAN and Rajesh MISHRA. The chemistry, manufacture, and tensile behavior of polyamide fibers. In: Anthony R. BUNSELL, ed. *Handbook of Properties of Textile and Technical Fibres* [online]. B.m.: Woodhead Publishing, 2018, The Textile Institute Book Series, s. 367–419. [accessed 2020-07-13] ISBN 978-0-08-101272-7. Available at: doi:10.1016/B978-0-08-101272-7.00012-2

11. List of papers published by the author

11.1. Publications in journals (Main author)

[1] **SIDDIQUE, Hafiz Faisal**, Zdeněk KŮS, Jiří MILITKÝ, Antonin HAVELKA, Adnan Ahmad MAZARI and Lubos HES. Development of new mathematical models and their comparison with existing models for the prediction of compression pressure using the cut-strip method. *Textile Research Journal* [online]. 2022, 00405175221088747. Available at: doi:10.1177/00405175221088747. **(Impact factor =2.455)**

[2] **SIDDIQUE, Hafiz Faisal**, Adnan Ahmed MAZARI, Antonín HAVELKA, Zdeněk KŮS a Engin AKCAGUN. Washing characterization of compression socks. *AUTEX Research Journal* [online]. 2022. ISSN 2300-0929. Available at: doi:10.2478/aut-2022-0009. **(Impact factor =1.944)**

[3] **SIDDIQUE, Hafiz Faisal**, Adnan Ahmed MAZARI, Antonin HAVELKA, Zdeněk KŮS, David CIRKL and Lubos HES. New approach for the prediction of compression pressure using the cut strip method. *Textile Research Journal* [online]. 2020, 90(15–16), 1689–1703. Available at: doi:10.1177/0040517519896757. **(Impact factor =2.455)**

[4] **SIDDIQUE, Hafiz Faisal,** Adnan Ahmed MAZARI, Antonin HAVELKA and Zdeněk KŮS. Performance characterization of compression socks at ankle portion under multiple mechanical impacts. *Fibers and Polymers* [online]. 2019, 20(5), 1092–1107. Available at: doi:10.1007/s12221-019-8965-1. **(Impact factor =2.153)**

[5] **SIDDIQUE, Hafiz Faisal**, Adnan MAZARI and Muhammad TANVEER. Sweat-management properties of semi bleached-socks using different main yarn and plating yarn combinations. *Fibres and Textiles* [Online]. 2019, **27**(1), 69–75. ISSN 1335-0617. **(Cite score =0.80)**

[6] **SIDDIQUE, Hafiz Faisal**, Adnan Ahmed MAZARI, Antonin HAVELKA and Zdeněk KŮS. Performance characterization and pressure prediction of compression socks. *Fibers and Polymers* [online]. 2020, 21(3), 657–670. Available at: doi:10.1007/s12221-020-9420-z. **(Impact factor =2.153)**

[7] **SIDDIQUE, Hafiz Faisal,** Adnan Ahmed MAZARI, Antonín HAVELKA and Radka LAURINOVÁ. Analysis of thermal properties affected by different extension levels of compression socks. *Fibres and Textiles* [Online]. 2019, 64–69. ISSN 1335-0617. **(Cite score =0.80)**

[8] **SIDDIQUE, Hafiz Faisal**, Adnan Ahmed MAZARI, Antonin HAVELKA, Tariq MANSOOR, Azam ALI and Musaddaq AZEEM. Development of V-shaped compression socks on conventional socks knitting machine. *Autex Research Journal*. [online]. 2018, 18, 377–384. Available at: doi:10.1515/aut-2018-0014. **(Impact factor =1.944)**

[9] **SIDDIQUE, Hafiz Faisal**, Adnan Ahmed MAZARI, Antonin HAVELKA, Sajid HUSSAIN and Tariq MANSOOR. Effect of elastic elongation on compression pressure and air-permeation of compression socks. *Fibres and Textiles* [Onlinee]. 2018, 1, 35–43. ISSN 1335-0617. **(Cite score =0.80)**

[10] **SIDDIQUE, Hafiz Faisal**. Assessment of mechanical properties of compression socks using cut-strip method. *Journal of Textile Engineering & Fashion Technology* [online]. 2019, 5(5). ISSN 2574-8114. Available at: doi:10.15406/jteft. 2019.05.00206.

[11] **SIDDIQUE, Hafiz Faisal**, Musaddaq AZEEM, Tanveer HUSSAIN, Azam ALI, Tariq MANSOOR and Amal BOUGHATTAS. Effect of elastane linear density on compression pressure of V-shaped compression socks. *Industria textila* [online]. 2018, 69(2), 118–127. Available at: doi:10.35530/IT.069.02.1433. **(Impact factor =0.823)**

11.2. Publications in journals (Co-author)

[1] AZEEM, Musaddaq, Amal BOUGHATTAS, **Hafiz Faisal SIDDIQUE**, Antonin HAVELKA, and Sajid HUSSAIN. Comfort properties of nano-filament polyester fabrics: Sensory evaluation. *Industria Textila* [online]. 2018, 69(1),3-10. Available at: doi: 10.35530 /it.069.01. 1440. **(Impact factor =0.823)**

[2] AZEEM, Musaddaq, Zuhaib. AHMAD, Jakub WIENER, Ahmad. FRAZ, **Hafiz Faisal SIDDIQUE** and Antonin HAVALKA. Influence of weave design and yarn types on mechanical and surface properties of woven fabric. *Fibres and Textiles in Eastern Europe* [online]. 2018, **26**(1). ISSN 12303666. Available at: doi:10.5604/01.3001.0010.7795.

(Impact factor = 1.045)

[3] KHAN, Muhammad Zaman, Sajid HUSSAIN, **Hafiz Faisal SIDDIQUE**, Vijay BAHETI, Jiri MILITKY, Musaddaq AZEEM, and Azam ALI. Improvement of liquid moisture management in plaited knitted fabrics. *Tekstil ve Konfeksiyon* [online]. 2018, 28(3), 182-188. **(Impact factor = 0.692)**

[4] MANSOOR, Tariq, Lubos HES, Zenun SKENDERI, **Hafiz Faisal SIDDIQUE**, Sajid HUSSAIN, and Asif JAVED. Effect of preheat setting process on heat, mass and air transfer in plain socks. *The Journal of the Textile Institute* [online]. 2019, 110(2), 159-170. Available at: doi: 10.1080/00405000.2018.1523990. **(Impact factor = 2.17)**

[5] MANSOOR, Tariq, **Hafiz Faisal SIDDIQUE**, Azam ALI, Petra KOMARKOVA, Antonin HAVELKA, and Zahid HUSSAIN. Wrinkle free plaited knitted fabrics without pre-heat setting. *Journal of the Textile Institute* [online]. 2018, 109(3), 307-311. Available at: doi: 10.1080/00405000.2017.1342585. **(Impact factor = 2.17)**

11.3. Contribution in the conference proceeding

[1] **SIDDIQUE, Hafiz Faisal**, Adnan Ahmed MAZARI, Antonín HAVELKA and Zdenek KŮS. Mathematical model for the prediction of compression pressure. 2019.

[2] **SIDDIQUE, Hafiz Faisal**, Adnan Ahmed MAZARI, Antonin HAVELKA and Zdeněk KŮS. Incorporation of some new parameters and modification of Laplace's law for prediction of compression pressure. In: . B.m.: PhD Day at Technical University of Liberec, 2019.

[3] **SIDDIQUE, Hafiz Faisal**, Adnan Ahmed MAZARI, Antonin HAVELKA and Zdeněk KŮS. New approach for the prediction of compression pressure using cut-strip method. In: Conference Fiber Society (proceeding), The University of Austin in Texas. 2019.

[4] **SIDDIQUE, Hafiz Faisal**, Adnan Ahmed MAZARI, Antonín HAVELKA and Zdeněk KŮS. Study of Performance Measurement of Compression Socks. In: Nanofibers, applications and related technologies–NART. 2019.

[5] **SIDDIQUE, Hafiz Faisal**, Adnan Ahmed MAZARI and Antonín HAVELKA. Thermal properties of compression socks at various extension levels. In: 18th AUTEX world textile

conference. 2018.

[6] **SIDDIQUE, Hafiz Faisal,** Zdeněk KŮS and Adnan Ahmed MAZARI. Effect of Extensibility on Compression Pressure and Air-Permeation in Compression Socks. In: . Technical University of Liberec: Technical University of Liberec, 2017.

[7] NAEEM, Jawad, Adnan Ahmed MAZARI, Michal KREJCIK and **Hafiz Faisal SIDDIQUE**. Impact of metallic coating on thermal protective behavior of multilayer protective clothing. In: Nanofibers, applications and related technologies–NART. 2019.

[8] ALI, Azam, Vijaykumar BAHETI, Abdul JABBAR, Jiri MILITKY, Sundaramoorthy PALANISAMY, **Hafiz Faisal SIDDIQUE** and Daniel KARTHIK. Effect of jute fibre treatment on moisture regain and mechanical performance of composite materials. In: IOP Conference Series: Materials Science and Engineering [online]. B.m.: IOP Publishing, 2017, s. 042001. Available at: doi:10.1088/1757-899X/254/4/042001

12. Research projects

1. Project leader SGS-19 (21309), Functional characterization of textile garments to improve their overall performance characteristics, Faculty of Textile Engineering, Technical University of Liberec, Czech Republic.
2. Member of SGS-18 (21246), Comfort and durability of compression socks, way of involvement, Faculty of Textile Engineering, Technical University of Liberec, Czech Republic

13. Citations

SIDDIQUE, Hafiz Faisal, Adnan Ahmed MAZARI, Antonin HAVELKA, Tariq MANSOOR, Azam ALI and Musaddaq AZEEM. Development of V-shaped compression socks on conventional socks knitting machine. *Autex Research Journal*. [online]. 2018, 18, 377–384. Available at: doi:10.1515/aut-2018-0014. **(Impact factor =1.944)**

Cited in 8 articles

SIDDIQUE, Hafiz Faisal, Adnan Ahmed MAZARI, Antonin HAVELKA, Zdeněk KŮS, David CIRKL and Lubos HES. New approach for the prediction of compression pressure using the cut strip method. *Textile Research Journal* [online]. 2020, 90(15–16), 1689–1703. Available at: doi:10.1177/0040517519896757. **(Impact factor =2.455)**

Cited in 5 articles

SIDDIQUE, Hafiz Faisal, Adnan Ahmed MAZARI, Antonin HAVELKA and Zdeněk KŮS. Performance characterization and pressure prediction of compression socks. *Fibers and Polymers* [online]. 2020, 21(3), 657–670. Available at: doi:10.1007/s12221-020-9420-z. **(Impact factor =2.153)**

Cited in 3 articles

SIDDIQUE, Hafiz Faisal, Adnan Ahmed MAZARI, Antonin HAVELKA, Sajid HUSSAIN and Tariq MANSOOR. Effect of elastic elongation on compression pressure and air-permeation of compression socks. *Fibres and Textiles* [Online]. 2018, 1, 35–43. ISSN 1335-0617. **(Cite score =0.80)**

Cited in 4 articles

SIDDIQUE, Hafiz Faisal, Adnan Ahmed MAZARI, Antonin HAVELKA and Zdeněk KŮS. Performance characterization of compression socks at ankle portion under multiple mechanical impacts. *Fibers and Polymers* [online]. 2019, 20(5), 1092–1107. Available at: doi:10.1007/s12221-019-8965-1. **(Impact factor =2.153)**

Cited in 2 articles

SIDDIQUE, Hafiz Faisal, Adnan Ahmed MAZARI, Antonín HAVELKA and Radka LAURINOVÁ. Analysis of thermal properties affected by different extension levels of compression socks. *Fibres and Textiles* [Online]. 2019, 64–69. ISSN 1335-0617. **(Cite score =0.80)**

Cited in 1 article